Canadian Journal of Earth Sciences

OPEN ACCESS | Research Article

New information on the holotype of "*Chasmosaurus*" *russelli* (Ornithischia: Ceratopsidae) necessitates the establishment of a new genus to receive the species

Robert B. Holmes[a], **Jordan C. Mallon**[a,b], **Michael J. Ryan**[a,b], **and David C. Evans**[c,d]

[a]Beaty Centre for Species Discovery and Palaeobiology Section, Canadian Museum of Nature, Ottawa, ON K1P 6P4, Canada; [b]Department of Earth Sciences, Carleton University, Ottawa, ON K1S 5B6, Canada; [c]Department of Natural History, Royal Ontario Museum, Toronto, ON M5S 2C6, Canada; [d]Department of Ecology and Evolution, University of Toronto, Toronto, ON M5S 3B2, Canada

Corresponding author: **Robert B. Holmes** (email: rholmes@nature.ca)

Abstract

Although the holotype of *Chasmosaurus russelli* Sternberg, 1940, from the upper Dinosaur Park Formation of southern Alberta, shares features with other *Chasmosaurus* Lambe, 1914 specimens from Dinosaur Provincial Park as well as various chasmosaurine taxa from the southwest United States, it also possesses unique features of the premaxilla and frill epiossifications. An iterative phylogenetic analysis, scoring only the holotype (CMNFV 8800), produces three consensus topologies, one of which places CMNFV 8800 closer to *Chasmosaurus* than to *Pentaceratops*, another in which CMNFV 8800 is closer to *Pentaceratops* than to *Chasmosaurus*, and a final topology in which these relationships are unresolved. Under current definitions, CMNFV 8800 cannot be accommodated within *Chasmosaurus* or any other known chasmosaurine genus. Consequently, we erect *Cryptarcus* gen. nov. to receive it. *Cryptarcus russelli* comb. nov. may represent a migrant originating from the southern "*Pentaceratops* clade", but it may also be part of a lineage more closely related to *Chasmosaurus* in which *Pentaceratops*-like features (e.g., frill wider anteriorly than posteriorly, deep parietal embayment, and first epiparietals nearly touch at the midline) evolved convergently. None of our phylogenetic topologies support an anagenetic trend from *Cryptarcus russelli* through *Pentaceratops* to produce *Terminocavus* Fowler and Freedman Fowler, 2020, as has been recently hypothesized.

Key words: *Cryptarcus*, *Chasmosaurus*, Chasmosaurinae, Ceratopsidae, Campanian, Dinosaur Park Formation

Introduction

The ceratopsid (horned) dinosaur clade Chasmosaurinae became established in North America by the middle Campanian (Longrich 2013) and diversified rapidly in the late Campanian. These animals are characterized by their intricate premaxillae, their often-lengthy postorbital horncores, and their posteriorly extended and variably ornamented parietosquamosal frills. The ingroup relationships of the subfamily Chasmosaurinae have never been firmly established. Traditionally, the genera comprising the Chasmosaurinae were though to have arisen sequentially, forming a Hennigian comb, with various species of *Chasmosaurus* Lambe 1914 diverging early in the history of the subfamily (e.g., Lehman 1996), but more recent phylogenetic assessments (e.g., Mallon et al. 2011) have hypothesized a deep split within the clade, with one lineage containing *Chasmosaurus* and its nearest relatives and the other containing *Triceratops* Marsh, 1889 and more closely related species.

Although five species of *Chasmosaurus*, including *Chasmosaurus belli* (as *Monoclonius belli* Lambe 1902), *Chasmosaurus canadensis* (as *M. canadensis* Lambe 1902), *Chasmosaurus brevirostris* Lull 1933, *Chasmosaurus kaiseni* Brown 1933, and *Chasmosaurus russelli* Sternberg 1940 had long been recognized, subsequent revision of the genus (Godfrey and Holmes 1995) indicated that only two of these (*C. russelli* and *C. belli*) are valid. More recently, *Chasmosaurus mariscalensis* Lehman 1989 was described (Lehman 1989); however, it has since been reassigned to the genus *Agujaceratops* (Lucas et al. 2006). In 2001, Holmes et al. described *Chasmosaurus irvinensis* Holmes, Forster, Ryan, and Shepherd 2001. This species was later transferred to *Vagaceratops* (Sampson et al. 2010). Although the latter reassignment generally has been accepted, at least one subsequent analysis (Campbell et al. 2016) has questioned its removal from *Chasmosaurus*. Longrich (2010) reassigned some specimens previously attributed to *Chasmosaurus russelli* to a new genus and species, *Mojoceratops perifania* Longrich, 2010, but this has not gained wide acceptance (Maidment and Barrett 2011; Mallon et al. 2011; Konishi 2015; Campbell et al. 2016; Fowler and Freedman Fowler 2020).

The phylogenetic relationships and, indeed, integrity of *C. russelli* have also recently been questioned (Fowler and Freedman Fowler 2020). The species was originally erected

by Sternberg (1940) based on a cranium (CMNFV 8800) collected southeast of the hamlet of Manyberries in southeastern Alberta (Sternberg 1940) from deposits later deemed to be equivalent in age to the lower Dinosaur Park Formation (Godfrey and Holmes 1995). Sternberg (1940) also designated a paratype (CMNFV 8801, a skull lacking a frill) and referred two additional specimens, CMNFV 8802 (a fragmentary skull) and CMNFV 8803 (a partial parietal), to the hypodigm. However, the first two specimens show no diagnostic features at the species level and are probably best referred to as *Chasmosaurus* sp. (Campbell et al. 2016). CMNFV 8803, although distinctive, is difficult to interpret, and its affinities are presently uncertain (Fowler and Freedman Fowler 2020, supporting information 1). Several additional specimens, all from the lower Dinosaur Park Formation of Alberta (Ryan and Evans 2005), were subsequently referred to *C. russelli* (Godfrey and Holmes 1995). However, it has become clear that the recently rediscovered holotype quarry is in the upper Dinosaur Park Formation (Campbell et al. 2016; Figs. 1 and 2), so CMNFV 8800 is considerably younger than all other material referred to *C. russelli*. This would confer upon the species a fossil history spanning most of the Dinosaur Park Formation (see, for example Campbell et al. 2016, fig. 4), which represents nearly 1.5 million years (Ramezani et al. 2022). Since megaherbivore turnover within the Dinosaur Park Formation was rapid, with species typically spanning 300–600 ka (Mallon et al. 2012; Eberth et al. 2023), this would represent an unusual species longevity for a member of this quickly evolving fauna. This has caused some to question whether any of the material from the lower Dinosaur Park Formation traditionally referred to *C. russelli* (e.g., Godfrey and Holmes 1995) is conspecific with the holotype (Fowler and Freedman Fowler 2020).

Phylogenetic analyses have recovered *Chasmosaurus russelli* as closely allied to the genotype species *Chasmosaurus belli* (e.g., Sampson et al. 2010; Mallon et al. 2011; Campbell et al. 2016; Knapp et al. 2018; Fowler and Freedman Fowler 2020). However, it is not always clear which specimens were used to establish character states in *C. russelli*. If these were taken from a mix of specimens selected from the hypodigm rather than exclusively from the holotype, then given that most—if not all—of the specimens traditionally included in the hypodigm are likely not conspecific with the holotype of *C. russelli*, it is possible that codings used in these phylogenetic analyses are chimeric. Most recently, Loewen et al. (2024, figs. S2 and S4), in a greatly expanded cladistic analysis that incorporated many new characters, recovered *C. russelli* as closer to *Pentaceratops* Osborn 1923 than to *C. belli* (to facilitate discussion, we will informally refer to all taxa more closely related to *Pentaceratops* than to *Chasmosaurus* as the "*Pentaceratops* clade"). In recent phylogenetic analyses, the "*Pentaceratops* clade" typically included, in addition to *Pentaceratops*, *Agujaceratops* Lucas, Sullivan, and Hunt, 2006, *Utahceratops gettyi* Sampson, Loewen, Farke, Roberts, Forster, Smith, and Titus 2010, *Navajoceratops* Fowler and Freedman Fowler 2020, and *Terminocavus* Fowler and Freedman Fowler, 2020. Significantly, the analysis of Loewen et al. (2024) places *C. russelli* within the "*Pentaceratops* clade". Although Loewen et al. (2024) took the character states for *C. russelli* primarily from the holotype, two additional specimens were also used. One of these, a partial parietal (TMP 2013.019.0038), also collected in the Onefour area, is plausibly attributable to this species. The other specimen (CMNFV 8801), originally designated a paratype of *C. russelli* by Sternberg (1940), lacks a frill, so the key diagnostic characters of the species cannot be confirmed. In addition, it was collected in what is now Dinosaur Provincial Park from deposits much older than those in the Onefour area, where the holotype was discovered (Figs. 1 and 2). Consequently, its assignment to *C. russelli* is problematic, and we have elected to exclude it from further consideration.

To address the issues concerning the diagnosis, hypodigm, and relationships of *C. russelli*, we revised the description of the holotype (CMNFV 8800), made any necessary revisions to the character codings based solely on this specimen, and reran the phylogenetic analysis of Loewen et al. (2024) to reassess its placement within the Chasmosaurinae. Our results suggest that the assignment of this specimen to *Chasmosaurus* is problematic at best, and we therefore erect a new genus, *Cryptarcus* gen. nov., to receive it.

Materials and methods

Old paint was removed from CMNFV 8800 using acetone and a soft brush to more clearly define sutures, surface sculpturing, and extent of plaster reconstruction. Fine preparation using mounted needle was performed. The skull was then photographed using a Canon EOS Rebel T1i, and a reconstruction was rendered on Strathmore Bristol using a Koh-I-Noor Rapidograph 0.35 mm drafting pen.

To assess the phylogenetic relationships of CMNFV 8800, we coded the cranium into the character matrix of Loewen et al. (2024) (Supplementary File Table S1). We chose this matrix for its recency and extensive character and taxon sampling. This is the first dataset that resulted in *Chasmosaurus russelli* being recovered as closer to *Pentaceratops sternbergii* Osborn, 1923 than to *Chasmosaurus belli*. As such, our redescription of the *C. russelli* holotype offers a timely opportunity to test this recent hypothesis. We note, however, that the matrix provided by Loewen et al. (2024) in their supplementary files is not the same as that used to produce all their own cladograms; *Coahuilaceratops magnacuerna* Loewen, Sampson, Lund, Farke, Aguillón-Martínez, De Leon, Rodríguez, and Eberth 2010 is missing, despite appearing in the cladogram presented in their Fig. S2. It was thus not possible to replicate their analyses precisely. Additionally, we modified character 355 (epiparietal, ep1 length) of Loewen et al. (2024), which they described as: state (1), "elongate, forms spike". However, as written, such a description makes no sense in light of their scorings, because many of the taxa scored (1) for this character (e.g., "*Mojoceratops*", *Utahceratops*) do not, in fact, have a parietal spike (defined by those authors in their supplementary character list as an ornamentation "more than 4 times longer than wide") at the ep1 locus. Instead, we interpreted this state to read "elongated into either a triangle, hook or spike", as used elsewhere to describe epiparietals ep2 and ep3 (i.e., characters 361:1 and 368:1). This revised description is consistent with the authors' original scorings.

Fig. 1. Locality photographs of CMNFV 8800, holotype of *Cryptarcus* ("*Chasmosaurus*") *russelli*. (A and B) Historic photographs of the quarry during excavation of CMNFV 8800 overseen by L. Russell; (C) southward-looking view of the exposures where CMNFV 8800 was collected. The sandstone layer in the middle of the sections hosted the specimen, but the quarry in not directly visible in this image; (D) quarry site of CMNFV 8800 in the foreground, looking southwards. Note the quarry stake is surrounded by a pile of rocks; (E) close up view of the head of the historic quarry maker labelled "Fossil Local 126 GSC 1" emplaced by C. M. Sternberg in 1937.

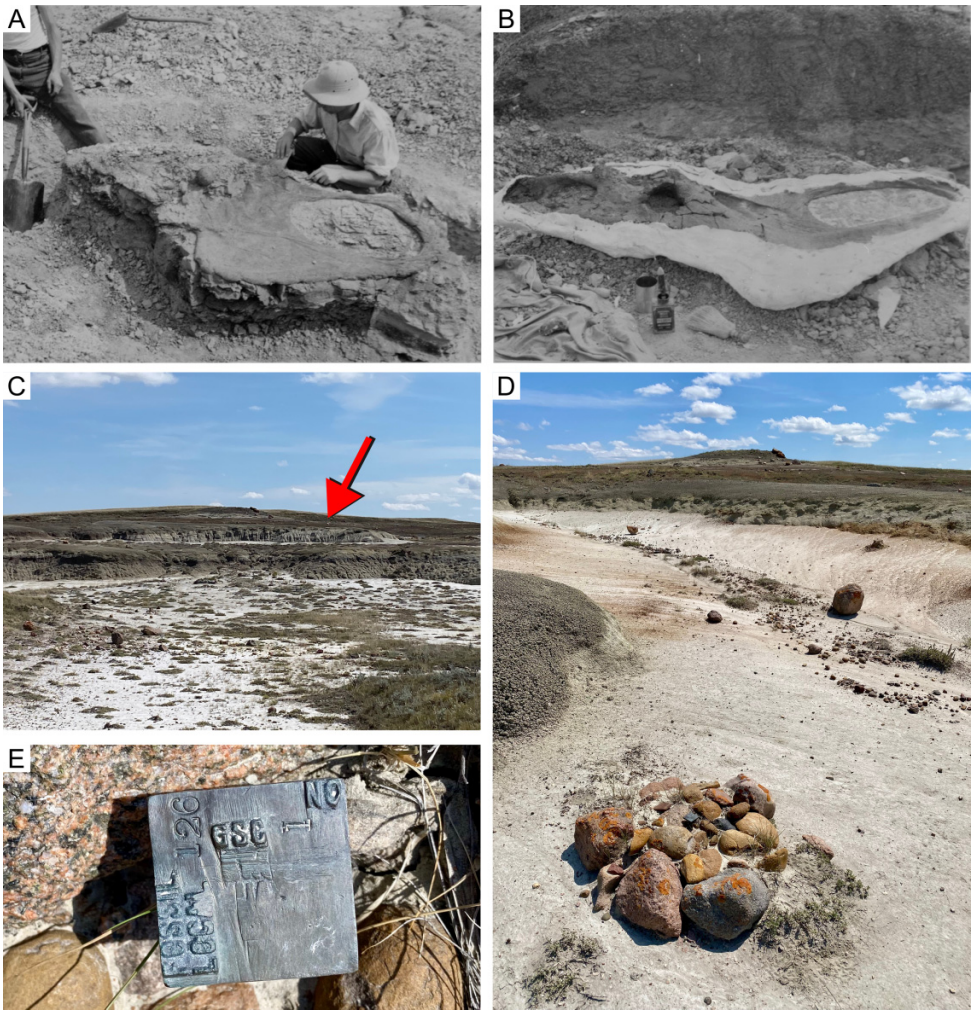

Because Loewen et al. (2024) included more than just the holotype in their coding of *Chasmosaurus russelli*, and given the problematic nature of some of these additional specimens (see Introduction for further details), we recoded the operational taxonomic unit with sole reference to CMNFV 8800 (Supplementary File Table S1). It was possible to code the specimen for 164 of 377 characters (45.3%) included in the matrix of Loewen et al. (2024). We found it necessary to modify the coding of 53 of these characters, either as a result of our reassessment of its anatomy or because the anatomy was not preserved. In addition, we recoded character 71 (nasal, ornamentation position, measured perpendicular to the toothrow) for *Pentaceratops sternbergii*; whereas this species was originally coded by Loewen et al. (2024) as "0" (centered posterior to anterior end of toothrow), the holotype skull (AMNH FR 6325) shows very clearly that the horn is centered anterior to the toothrow, so it was recoded as "1". We did not otherwise attempt to verify the codings for the remaining taxa in the matrix.

We further modified the matrix by coding the recently described chasmosaurine *Navajoceratops sullivani* (Fowler and Freedman Fowler 2020), which we felt necessary due to the original authors' argument that it is closely allied to the "*Pentaceratops* clade" and may, therefore, affect the placement of CMNFV 8800. We did not add their newly coined *Terminocavus sealeyi*, because the holotype of that species (NMMNH P-27468) was already included in the coding for *P. sternbergii* by Loewen et al. (2024).

Finally, we appended a new character (378. Epiparietal, ep1 spacing: [0] ep1 episossifications separated along transverse parietal bar by distance greater than or equal to basal length of ep1; [1] ep1 ossifications separated along transverse parietal bar by distance less than basal length of epiparietal ep1) to the matrix, recognizing the fact that, in some skulls (e.g., CMNFV 8800, *Utahceratops*, *Anchiceratops ornatus* Brown 1914), the first epiparietals abut on the midline or nearly so.

We conducted a series of parsimony-based cladistic analyses using a variety of assumptions to test stability of the

Fig. 2. Spatiotemporal context of *Cryptarcus* ("*Chasmosaurus*") *russelli* gen. nov. holotype (CMNFV 8800) and referred material (TMP 2013.018.0038). (A) map of southern Alberta showing location of holotype and referred material (red star); (B) geological map showing stratigraphic positions of CMNFV 8800 and referred specimen. Radioisotopic dates in B after Ramezani et al. (2022). The Onefour section is a schematic that summarizes data from Eberth and Brinkman (1997), Eberth (2024), and DCE (this study).

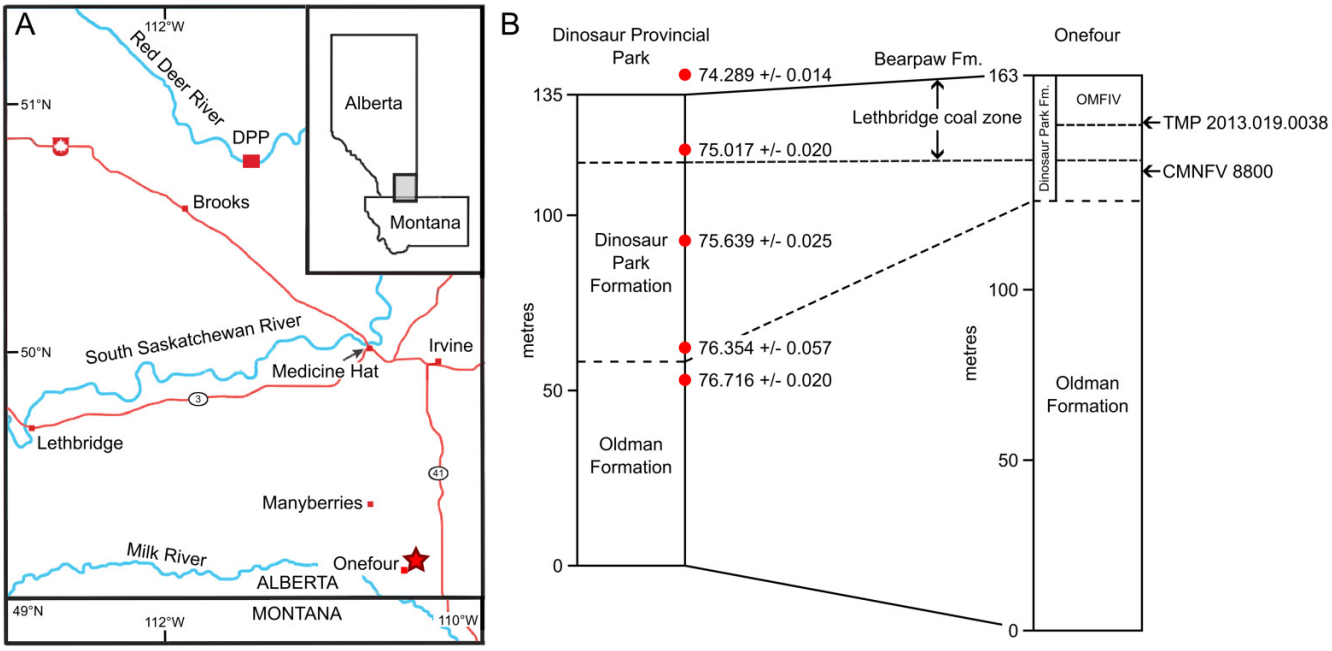

Table 1. Settings used for iterative cladistic analysis.

Iteration	Weighting type	Weighting function (*K*) value	Characters 339 and 340 excluded?
1	None	NA	Yes
2	None	NA	No
3	Implied weighting	3	Yes
4	Implied weighting	12	Yes
5	Extended implied weighting	3	Yes
6	Extended implied weighting	12	Yes

Note: See the text for invariant settings. The weighting function (*K*) was allowed to vary between 3 and 12, per Goloboff et al. (2018).

phylogenetic position of CMNFV 8800. The variable assumptions generally concerned the inclusion or exclusion of certain characters, the application of implied and extended implied weighting (Goloboff 2014), and variations of the weighting function. The details of each iteration are given in Table 1. Early testing showed that traditional search settings consistently outperformed "new technology" searches (i.e., recovered more most parsimonious trees of shorter length), so we report the results of only the former here. We conducted all analyses in TNT v. 1.5 (Goloboff and Catalano 2016). In every iteration, we maximized the number of trees held in memory (99 999) and specified *Hypsilophodon foxii* Galton 1974 as the outgroup. Following Loewen et al. (2024), characters 1, 51, 70, 126, 130, 144, 170, 261, 262, 279, and 336 were designated as additive. In most iterations, characters 339 and 340 (relating to the flattening of epiparietal spikes) were excluded, because this same information is captured by characters 355 and 356 (relating to the ep1 epiparietal), and characters 363 and 364 (relating to the ep2 epiparietal). Our traditional searches specified Wagner starting trees (random seed of "0" with 1000 replications) and a tree bisection-reconnection swapping algorithm (100 trees saved per replication). Bootstrap clade support was generated in TNT, specifying 10 000 replicates and a traditional tree-search algorithm. Values are reported as absolute frequencies.

Institutional abbreviations

AMNH, American Museum of Natural History, New York, New York, USA; **CMNFV**, Canadian Museum of Nature (Fossil Vertebrates), Ottawa, Ontario, Canada; **NHMUK**, Natural History Museum, London, UK; **ROM**, Royal Ontario Museum, Toronto, Ontario, Canada; **TMP**, Royal Tyrrell Museum of Palaeontology, Drumheller, Alberta, Canada; **UALVP,** Univer-

Fig. 3. *Cryptarcus* ("*Chasmosaurus*") *russelli* holotype cranium (CMNFV 8800). (A) Skull in left lateral view (with restored jugal and lower jaw); (B) detail of snout in left lateral view; (C) detail of parietosquamosal frill in dorsal view; (D) detail of supraorbital review in dorsal view; (E) detail of es6 episquamosal; (F) detail of es7 episquamosal. Arrowheads in E and F point to margins of episquamosals.

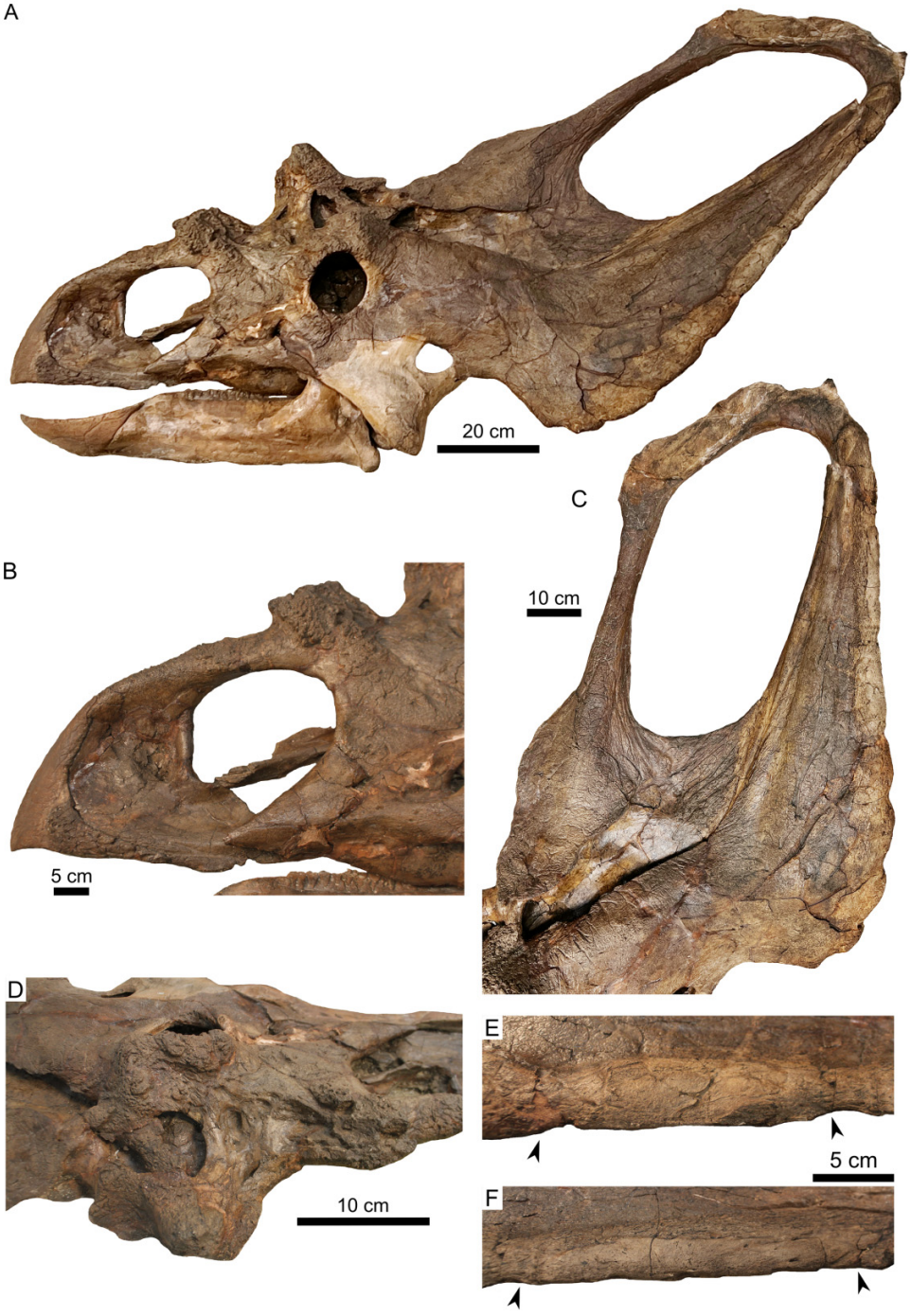

sity of Alberta Laboratory of Vertebrate Palaeontology, Edmonton, Alberta, Canada; **YPM**, Peabody Museum, Yale University, New Haven, Connecticut.

Systematic palaeontology

Ceratopsia Marsh, 1888
Neoceratopsia Sereno, 1986
Ceratopsidae Marsh, 1888
Chasmosaurinae Lambe, 1915

Cryptarcus gen. nov.
Cryptarcus russelli (Sternberg, 1940)
(Figs. 2 and 3)

ETYMOLOGY: From the Latin *crypticus* (hidden) and *arcus* (arch), referring to both to the morphology of the transverse partial

bar and to the fact that the type species was "hidden" within the genus *Chasmosaurus* since it was first named.

DIAGNOSIS: Chasmosaurine ceratopsid having the following autapomorphies (characters unique with respect to Chasmosaurinae): termination of posteroventral process of premaxilla spatulate and not tapering distally; bases of episquamosals becoming progressively longer in posterior direction until the second to most posterior (2nd) episquamosal, after which this trend is reversed, with the most posterior episquamosal (1st) being distinctly smaller than the 2nd; both epiparietals 1 and 2 have low, dome-shaped profiles with lenticular-shaped loci; epiparietals 1 and 2 fused (although the suture between them is visible); loci of epiparietals 1 and the medial portion of epiparietal 2 are located on the dorsal surface of the posterior parietal bar, with lateral portion of epiparietal 2 turning onto the posterior edge of the bar; differs from *Chasmosaurus* in possessing: an antorbital buttress that is restricted to the palpebral (shared with *Regaliceratops*); a parietosquamosal frill that, when viewed dorsally, appears wider anteriorly than posteriorly (shared with *Pentaceratops*, aff. *Pentaceratops* MNA Pl 1747, and *Utahceratops*); a deeply emarginate posterior frill margin (shared with *Pentaceratops*, aff. *Pentaceratops* MNA Pl 1747, *Utahceratops*, and *Agujaceratops*); medial-most epiparietals (1st) that nearly touch at the midline (shared with *Pentaceratops*, aff. *Pentaceratops* MNA Pl 1747, *Utahceratops,* and *Anchiceratops*); epiparietals 1 and 2 that are both located entirely within posterior parietal embayment (shared with aff. *Pentaceratops* MNA Pl 1747); lateral and dorsal margins of squamosal that are essentially straight, in contrast with *Agujaceratops*, in which the lateral margin is convex, resulting in a broad posterior blade, and the dorsal margin is more dorsally concave through most of its length, producing a more upright frill.

HOLOTYPE: CMNFV 8800, a mostly complete cranium exposed in left lateral view.

REFERRED MATERIAL: TMP 2013.019.0038, a partial parietal.

LOCALITY, HORIZON, AND AGE: The holotype of *Chasmosaurus russelli* (Figs. 1A and 1B) was collected in 1936 by Loris Russell from a small area of badlands in the extreme southeast corner of southern Alberta near the Onefour Research Station (now closed), 2.4 km north of a cluster of currently abandoned buildings located on the north side of Township Road 21A, and about 33 km southeast of the hamlet of Manyberries. In 1937, the quarry site was marked with a square-headed quarry stake engraved as GSC 126-1 by C. M. Sternberg (Fig. 1E). Outcrop in this area is patchy and limited in vertical extent, making stratigraphic interpretations challenging. One of us (DCE) visited the quarry site (Figs. 1C–1E) on 18 July 2025 and measured the full outcrop in the immediate area of the quarry marker. The section, taken from the creek bed ~200 m north of the quarry southwestward to the top of the hill above the site, measures 18 m thick and is composed predominantly of organic rich mudstones. The base of the section is defined by a 3 m thick, soft, gray-buff sandstone-dominated unit with inclined heterolithic strata. The specimen was collected from within a 1.5 m thick sandstone similar in appearance to the basal unit. It is laterally extensive in the area and highly fossiliferous, especially at its base. This host unit is separated from the basal sandstone unit by a 7.5 m layer of mudstones and overlain by a 1.5 m layer of mudstone, which is in turn capped by a 4.5 m sequence containing multiple, thin carbonaceous shale/lignite layers interpreted here as representing the bottom of the Lethbridge Coal Zone (LCZ). The entire section is interpreted to represent the Dinosaur Park Formation (DPFm). Eberth (2024) measured the DPFm to be 32 m thick in the Onefour area, of which only about 12 m of the DPFm occurs between the LCZ and the contact with the underlying Oldman Formation (Eberth 2024, fig. 5). This compares favourably with our measurement of 13.5 m of DPFm below the hypothesized base of the LCZ measured by DCE and suggests that the top of the Oldman Formation is covered but very close to the base of the quarry section. If this interpretation is correct, the host stratum of CMNFV 8800 is located between 1.5 and 3 m below the base of the Lethbridge Coal Zone, and within the middle of the DPFm in the general Onefour area.

The referred specimen, TMP 2013.019.0038, was also collected in strata of the DPFm in the Onefour area. The specimen was discovered and collected by Wendy Sloboda on 7 July 2013 on the Sage Creek Grazing Reserve, 5.7 km to the east of the CMNFV 8800 quarry, and at a similar stratigraphic level (Fig. 2). A highly fossiliferous, complex mud-filled incised valley system (OMFIV—see Brinkman and Eberth (1997)) spans the Onefour Heritage Rangeland Natural Area and the Sage Creek Grazing Reserve (Eberth 1996; Eberth and Brinkman 1997). TMP 2013.019.0038 was collected near the "Car Park Site" (Eberth and Brinkman 1997). Here, the outcrop is only ~17 m in thickness and is composed predominantly of the LCZ. We estimate that TMP 2013.019.0038 was collected from the basal lag of the incised valley fill, and therefore about 9 m above the base of the LCZ in this area (Eberth and Brinkman 1997). The incised nature of the depositional setting indicates that the stratigraphic position of TMP 2013.019.0038 relative to CMNFV 8800 is somewhat higher still, as its host unit was deposited in an incision cut down through older deposits of the LCZ.

Description of CMNFV 8800

CMNFV 8800 consists of an articulated cranium exposed in left lateral view (Figs. 2 and 3). With a basal skull length of ~940 mm (using the distance from anterior edge of rostral–posterior margin of the infratemporal opening as a proxy), it rivals the largest *Chasmosaurus* skulls in size (e.g., *C. belli* [ROM 839 = 810 mm, YPM 2016 = 848 mm, ROM 843 = ~1000 mm]; cf. *C. russelli* [CMNFV 2280 = 726 mm]). Most of the rostral, portions of the left orbital rim, ventral flange of the left jugal, left quadrate, left quadratojugal, right half of the frill, and lower jaws are missing and have been reconstructed in plaster. The left half of the frill, including the median parietal bar, has been rotated counterclockwise relative to the long axis of the skull and presents in dorsolateral aspect. It has been dorsoventrally flattened, causing the ventral edge of the squamosal to splay laterally, slightly exaggerating its anterior width in dorsal aspect (Fig. 3). The orbital region of the skull has been mediolaterally compressed,

Table 2. Select cranial measurements of the *Cryptarcus russelli* gen. nov. holotype (CMNFV 8800).

Measurement	Value(s) (left/right) (mm)
Postorbital horncore length (rectilinear) from skull roof to apex	?/89
Postorbital horncore anteroposterior length at base	?/132
Postorbital horncore mediolateral width at base	?/82
Postorbital horncore circumference about base	?/277
Nasal horncore height from base to apex (excluding nasal bridge)	89
Nasal horncore transverse width at base	105
Nasal horncore anteroposterior length at base	162
Rostral-orbit length	666 (est.)/?
Posterior margin of external naris-orbit length	218/?
Rostral-posterior margin of nasal horncore	587
Lateral temporal fenestra-orbit length	160/?
Orbit anteroposterior length	120/?
Orbit dorsoventral height	130/?
Minimum distance from jugal notch to medial margin of squamosal	254/?
Minimum distance from lateral margin of anterior-most episquamosal to medial margin of squamosal	331/?
Rostral-posterior edge of maxillary tooth row	752 (est.)/?
Basal skull length (rostral-middle of lateral temporal fenestra)	920 (est. using post. margin of lateral temporal fenestra)
Maximum anteroposterior length of skull (rostral-posterior parietal, excluding epiossifications)	2000
Length of squamosal from jugal notch to its distal end	1007/?
Maximum length of squamosal from apex of anterior-most episquamosal to distal end	1005/?
Jugal notch-parietal fenestra (curvilinear)	460/?
Posterior margin of frontoparietal fontanelle to posterior edge of medial parietal bar (curvilinear)	880
Proximal transverse width of frill (at episquamosal es3), measured along curved surface	1260 (est.)
Transverse width of frill at mid-length (midway between jugal notch and posterior margin), measured along curved surface	1040 (est.)
Transverse width of frill at posterior tip of squamosal, measured along curved surface	760 (est.)
Maximum length of parietal fenestra	620/?
Maximum width of parietal fenestra	291/?
Maximum skull length, rostral-epiparietosquamosal	1980
Jugal notch (from squamosal lateral corner) to apex of epiparietosquamosal	1090/?
Jugal notch (from squamosal lateral corner) to posterior margin of parietal (not including epiparietals)	1085/?
Occipital condyle-posterior margin of frill	1170

Note: Abbreviation: est., estimated.

and the left orbital region, including the left horncore, has been displaced anterodorsally, causing some plastic deformation of the snout. The bone texture over much of the external surface of the skull (e.g., dorsal premaxillary arch, lateral walls of the nasal, postorbitals, parietal and squamosals) is rugose and in some places heavily sulcated, which is typical of adult ceratopsids (Sampson et al. 1997; Brown et al. 2009). Long-grained bone texture diagnostic of young ceratopsids is entirely absent. Select cranial measurements are provided in Table 2. A 3D photogrammetric model of the skull is available via MorphoSource at https://doi.org/10.17602/M2/M723582.

Preorbital region

Most of the rostral is missing; only some of the central portion and the posteroventral process that extends along the ventral margin of the premaxilla are preserved. Sternberg (1940) used the lack of a "hooked" rostral as a diagnostic character of *Chasmosaurus russelli*. Although the straight ventral margin of the latter process gives no hint of the ventrally hooked lateral profile usually seen in chasmosaurines, the incompleteness of the element negates a definite assessment, so the lack of rostral hook was subsequently removed from the diagnosis (Godfrey and Holmes 1995). A facet on the anterodorsal surface of the premaxillae indicates that the missing posterodorsal process of the rostral also formed a discrete process; this would have resulted in the deeply concave posterior rostral border typical of chasmosaurines. The exposed left premaxilla is complete, although its posteroventral process has broken away from the rest of the bone ventral to the naris and has been displaced approximately 30 mm anterodorsally. The oval central fossa of the premaxillary septum is unperforated. The premaxillary fenestra is sometimes present in *Triceratops* (Forster 1996) and some other chasmosaurines (e.g., cf. "*Chasmosaurus*" *russelli* [CMNFV 2280], *Anchiceratops* Sternberg 1929 [CMNFV 8535],

Chasmosaurus belli [AMNH 5402]), but well-defined fenestra margins are rarely preserved, and in many cases these "fenestrae" may simply represent broken bone lost postmortem from the thinnest area of the septum. Immediately anterior to the naris, the septum forms a distinct narial strut. The posterior border of the strut is curved, obscuring its orientation, but the dorsal roof of the strut is located slightly posterior to its ventral base, producing a slight posterior tilt, similar to that described in *Spiclypeus shipporum* Mallon, Ott, Larson, Iuliano, and Evans 2016, *Kosmoceratops richardsoni* Sampson, Loewen, Farke, Roberts, Forster, Smith, and Titus 2010, and CMNFV 8801 (originally designated the paratype of *C. russelli* (Sternberg 1940), which was later referred to cf. *K. richardsoni* (Longrich 2014), but probably best relegated to *Chasmosaurus* sp. (Campbell et al. 2016)). In cf. "*C.*" *russelli* (CMNFV 2280 and TMP 1981.019.0175), *C. belli* (NHMUK R4948, Maidment and Barrett 2011), *Pentaceratops sternbergii* Osborn 1923 (AMNH 6325), and *Triceratops* spp. (Forster 1996), the narial strut is inclined anteriorly. In some chasmosaurines, the posterior margin of the strut bears a median flange that projects into the naris. This flange is not present in CMNFV 8800, but broken bone on the posterior margin of the strut suggests that its apparent absence may be an artifact of postmortem damage or incomplete preservation. A large, subrectangular endonarial process (="triangular process" of Lehman 1998, fig. 8) projects posteriorly from the base of the narial strut into the anteroventral corner of the naris. The posteroventral process of the premaxilla forms a broad lamina that overlaps the ventral part of the nasal, concealing the contribution of the latter to the posteroventral margin of the naris in lateral view. This is distinct from *Chasmosaurus*, in which the posteroventral process narrows posterodorsally to expose more of the lateral surface of the nasal. A small foramen pierces the side of the snout between the premaxilla and nasal. It occupies a position similar to that of the accessory antorbital fenestra present in basal neoceratopsians such as *Zuniceratops* Wolfe and Kirkland 1998, *Diabloceratops* Kirkland and DeBlieux 2010, and *Bagaceratops* Maryańska and Osmólska 1975 (Kirkland and Deblieux 2010). A similar foramen has been recorded in some chasmosaurines (e.g., cf. "*C.*" *russelli*, TMP 1981.019.0175 (Godfrey and Holmes 1995, fig. 2), AMNH 5401 (as "*Mojoceratops perifania*" (Longrich 2010, fig. 8), and a juvenile attributed to *C. belli* (Currie et al. 2016)), but is absent in most *Chasmosaurus* specimens (Campbell et al. 2016, supplementary material 2). The homology between this foramen and the accessory antorbital fenestra of basal ceratopsids has been questioned (Loewen et al. 2024). The posterodorsal process of the premaxillae is broadly expanded, much as in centrosaurines, and inserts into the bifurcated anterior process of the coossified nasals, although the overlap between nasals and premaxillae is limited, at least as exposed dorsally.

The short, stout, broad-based nasal horncore is heavily pitted and swollen. It appears to be truncated, but it is impossible to determine from external appearances whether this is the result of pathology or resorption. It is not possible to unequivocally identify an epinasal suture (but see Campbell et al. 2016, fig. 11*e* for an alternate interpretation). The posterior surface of the horncore bears deep, dorsoventrally oriented grooves. Similar grooves are seen on the nasal horncore of a long-horned *Chasmosaurus* skull (TMP 2015.018.0012) from the Dinosaur Park Formation near Hilda, Alberta, as well as on the nasal horncore and medial epiparietals of *Centrosaurus apertus* (Sternberg 1940; Frederickson and Tumarkin-Deratzian 2014; Mallon et al. 2023). The contours of the preserved anterior and posterior surfaces of the horncore stump suggest that the horncore, prior to its modification (whether as a result of pathology or resorption and remodeling) would have been inclined slightly anteriorly and would not have exceeded 200 mm in length (Fig. 4). Too little is preserved to determine if the complete horncore had been straight or curved. Approximately 50% of the nasal horncore base is located posterior to the external naris. This position is most similar to that in *K. richardsoni* (Sampson et al. 2010) and some *Chasmosaurus* (e.g., CMNFV 2280, NHMUK R4948, UALVP 40), but contrasts with the condition in *Pentaceratops* and *Triceratops*, where the nasal horncore is located entirely over the external naris, as well as the condition in *Utahceratops* and CMNFV 8801 (*Chasmosaurus* sp.), where the horncore is situated entirely behind the external naris (Sampson et al. 2010; Longrich 2014).

The maxilla contacts the lacrimal dorsally where it forms the anterior and ventral margins of a modestly sized antorbital fenestra. The posterior end of the superficial ramus is complete, but its contact with the jugal has been disrupted, and the adjoining portion of the jugal is missing. Immediately anterior to the exposed sutural contact, the ventral margin of the superficial ramus turns ventrally. The relatively straight ventral margin of the inset dental ramus of the maxilla is located slightly ventral to the oral margin of the premaxilla. None of the teeth are present, and the alveoli are not well enough preserved to allow an estimate of the tooth count. However, it is clear that there is a short "diastema" between the first alveolus and the anterior end of the bone, and that the toothrow extended to the posterior end of the dental ramus.

Circumorbital region

Coossificaton of the circumorbital bones is advanced so that most sutures between them cannot be clearly defined. Each postorbital bears a broad-based, oval horncore stump (slightly longer anteroposteriorly than transversely) located directly over the orbit. Like the nasal horncore, they show evidence of modification either as a result of pathology or resorption. As an ontogenetic series for this taxon does not exist, there is no unequivocal evidence for a hypothesis of resorption. However, by analogy with *Centrosaurus* (e.g., Sampson et al. 1997; Ryan et al. 2001; Fredrickson and Tumarkan-Deratzian 2014), in which ontogenetic resorption of orbital horncores has been established, a similar ontogenetic process in CMNFV 8800 is plausible. Sternberg (1940) argued that well-defined horncores are lacking. Although the left horncore is almost completely absent, the right horncore preserves more of its basal portion. Its contours suggest that it would have been inclined slightly anteriorly and was possibly as long as 250 mm. Because the skull is laterally crushed, it is not possible to determine whether the horncores were

Fig. 4. Restored cranium of the *Cryptarcus* ("*Chasmosaurus*") *russelli* holotype (CMNFV 8800). (A) Cranium in left lateral view; (B) cranium in dorsal view. Dashed lines denote restored elements. Abbreviations: enp, endonarial process; ep#, epiparietal identity; es#, episquamosal identity; f, frontal; fpf, frontoparietal fontanelle; j, jugal; na, nasal; nahc, nasal horncore; ns, narial strut; p, parietal; pf, parietal fenestra; pmx, premaxilla; pmxf, premaxillary fossa; po, postorbital; pohc, postorbital horncore; sq, squamosal; stf, supratemporal fossa.

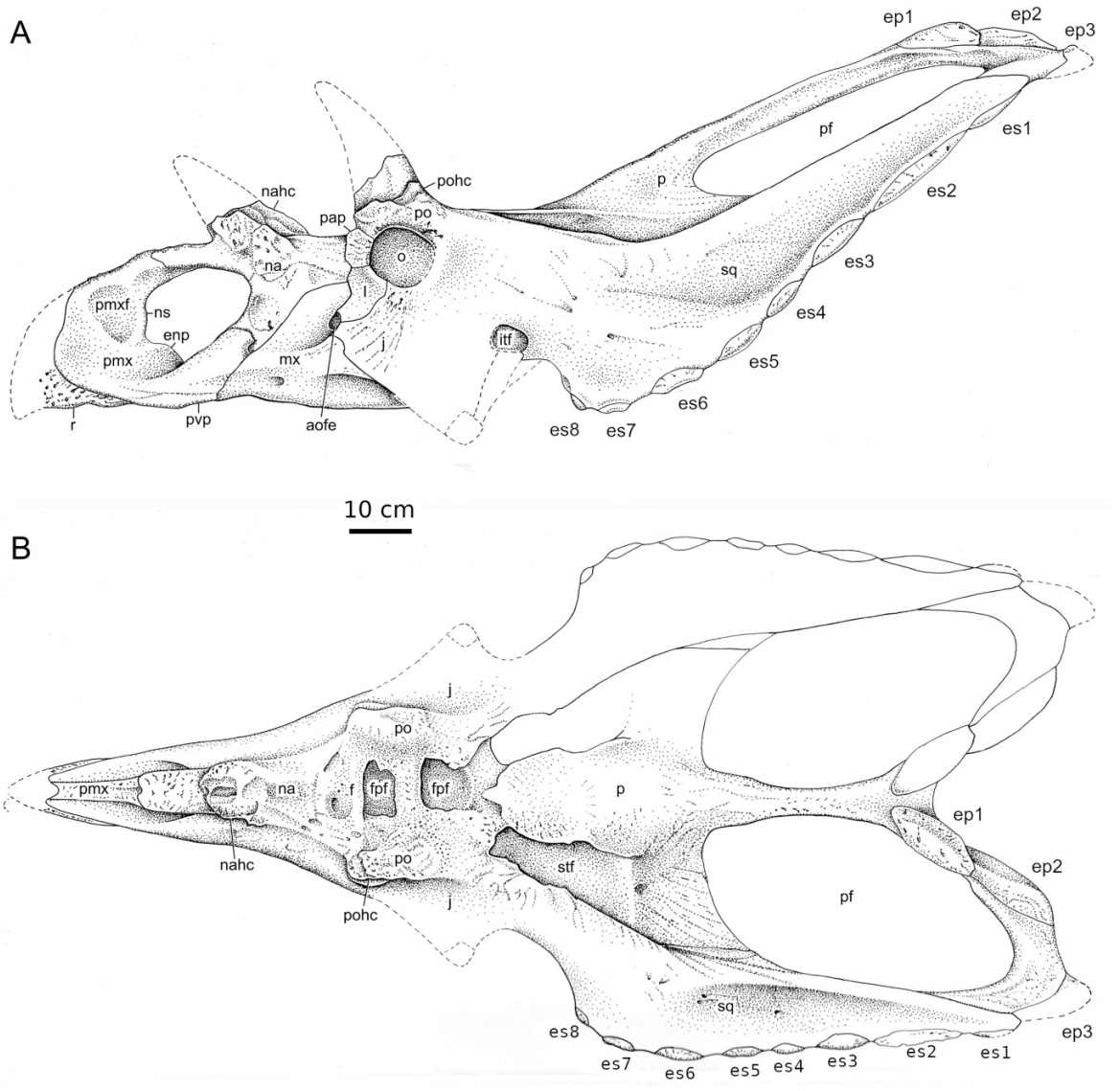

erect or diverged from the sagittal plane. A massive, isolated postorbital horncore (CMNFV 55193, Fig. 5C) collected from the Onefour area, likely from approximately coeval strata as CMNFV 8800, may be conspecific. Although it shares no diagnostic characters with the latter, it cannot be attributed to any other ceratopsid known from these deposits, and may represent a non-pathological specimen of this taxon, or an earlier ontogenetic stage in which the horncores had not yet begun the resorption process. Posterior to the horncore, each postorbital extends a lamina that overhangs the anterior end of the supratemporal fenestra. The ventral aspect of the postorbital is difficult to access, but the supracranial sinus does not appear to have extended into the base of the horncore, a morphology shared with CMNFV 55193.

The palpebral bears a prominent, rugose antorbital buttress. The precise location of the palpebral-lacrimal suture cannot be verified, because part of the anterior margin of the orbit in this region is missing and has been reconstructed in plaster. Preserved portions of both the lacrimal and adjacent jugal indicate that, although the bone adjacent to the orbit was thickened, there is no evidence that the antorbital buttress extended onto the lacrimal.

Below the orbit, the lacrimal forms an extensive contact with the anterior end of the jugal. Only the dorsal portion of the jugal, forming the ventral rim of the orbit, is preserved. However, the general shape of the bone can be estimated, because the ventrally turning posterior end of the preserved ventral margin of the superficial ramus of the max-

Fig. 5. Comparative material from near Onefour, Alberta. (A) *Cryptarcus* ("*Chasmosaurus*") *russelli* referred partial parietal (TMP 2013.019.0038) in dorsal view; (B) same in ventral view; (C) left postorbital horncore (CMNFV 55193) in lateral view, possibly referable to *Cr. russelli*; (D) same in medial view.

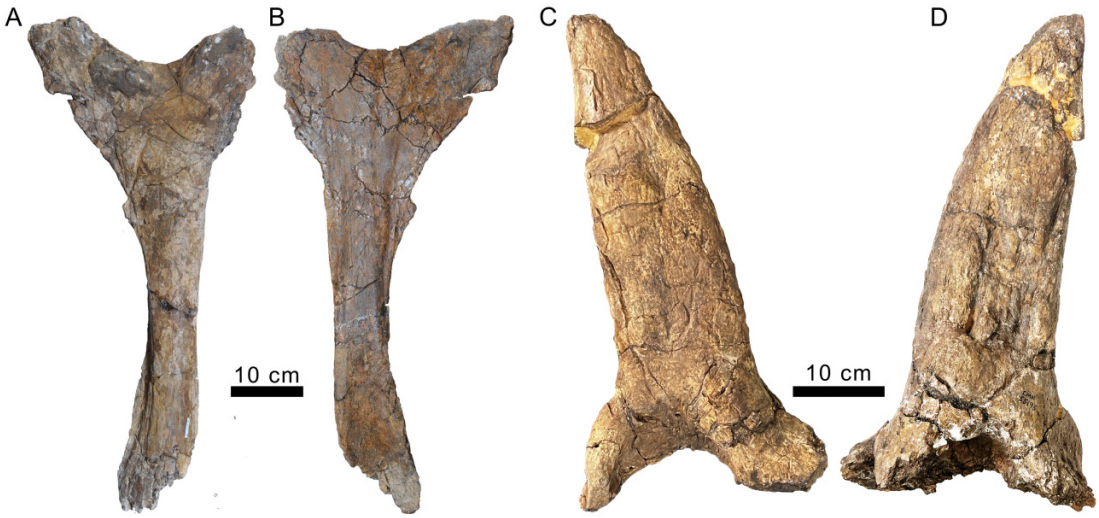

illa (see above) indicates that, as in *Chasmosaurus*, the complete jugal included a broad-based ventral triangular flange that would have concealed the posterior portion of the tooth-bearing ramus of the maxilla in lateral view (Fig. 3). This is in distinct contrast to the narrow-based jugal flange of *Agujaceratops mariscalensis* (as "*Chasmosaurus*" *mariscalensis* Lehman 1989), *Pentaceratops* (Lehman 1998), *Utahceratops*, *Kosmoceratops* (Sampson et al. 2010), and *Triceratops* (e.g., Ostrom and Wellnhofer 1986). In all cases except *Triceratops*, this narrow base fails to obscure any part of the dental ramus in lateral view.

Supraorbital region

The supraorbital region has been mediolaterally compressed during preservation, causing the right side of the skull to be displaced anteriorly relative to the left side, and partly collapsing the frontoparietal fontanelle, obscuring the shape of the opening. Nevertheless, it is clear that the fontanelle was unusually wide (approximately 95 mm at its greatest width anteriorly), irregular in shape, and apparently asymmetrical with respect to the midline (Fig. 3). It is divided into anterior and posterior halves by a broad transverse bridge of bone, apparently formed by the postorbitals. This condition is approached in some specimens in which the fontanelle narrows near its mid-length (e.g., CMNFV 2280, YPM 2016 (see Godfrey and Holmes 1995)) suggesting incipient bisection of the opening. The bridge seen in CMNFV 8800 appears to be an ontogenetic end point of this morphology. Coossification of sutures in this region appears to be advanced; as a consequence, the extent of the frontals and their specific relationships with the nasals and postorbitals are uncertain. However, the general morphology of the supraorbital region suggests that, as in other chasmosaurines (e.g., Lehman 1990), the frontals form no more than the overhanging anterior margin of the fontanelle. The dorsal surface of the skull anterior to the fontanelle (probably representing the frontals, prefrontals, and possibly the posterior part of the nasal) appears abnormal (Sternberg 1940). The bone surface is conspicuously unsculptured, and bears two large, apparently bilaterally symmetrical foramina (or fistulae?), as well as a number of other divots (some of which appear to be arranged bilaterally); in a few cases, these divots appear to lead into foramina (Fig. 3D). Such texturing, unknown on this region of the skull in ceratopsids, may be related either to the advanced age of the specimen or to pathology (e.g., osteomyelitis).

Parietosquamosal frill

As in other chasmosaurines (with the conspicuous exception of *Triceratops*), the parietosquamosal frill is long, measuring about 120% of basal skull length. As in all ceratopsids, the anterior portion of the frill, measured along its curved surface, is wider than the posterior portion of the frill (Table 1); however, as a result of a pronounced dorsal curvature of the anterior frill, this disparity between widths is minimized when viewed dorsally, and the anterior portion of the frill appears only slightly wider than the posterior frill in dorsal projection. These proportions are reminiscent of those in *Pentaceratops*, *Utahceratops*, and *Agujaceratops*, but distinct from *Chasmosaurus*, in which the frill, in rectilinear projection, appears to widen posteriorly to produce a distinctly fan-shaped outline (Fig. 6).

The parietal fenestra is large (Table 1) and approximately oval in outline. Its long axis diverges posteriorly at an angle of about 25° from the sagittal.

Typical of most chasmosaurines, the squamosal forms an elongate, scalene triangle. As in *Chasmosaurus* generally, its essentially straight lateral edge converges smoothly with the dorsal margin to form an acute posterior termination located immediately anterior to the arched posterior margin of the

Fig. 6. Comparison of chasmosaurine frills in dorsal view. *Agujaceratops mariscalensis*, *Utahceratops gettyi*, *Pentaceratops sternbergii*, aff. *Pentaceratops* n. sp., cf. *Chasmosaurus* russelli, and *Chasmosaurus belli* modified from Lehman (1989), Sampson et al. (2010), Longrich (2014), Rowe et al. (1981), and Godfrey and Holmes (1995), respectively.

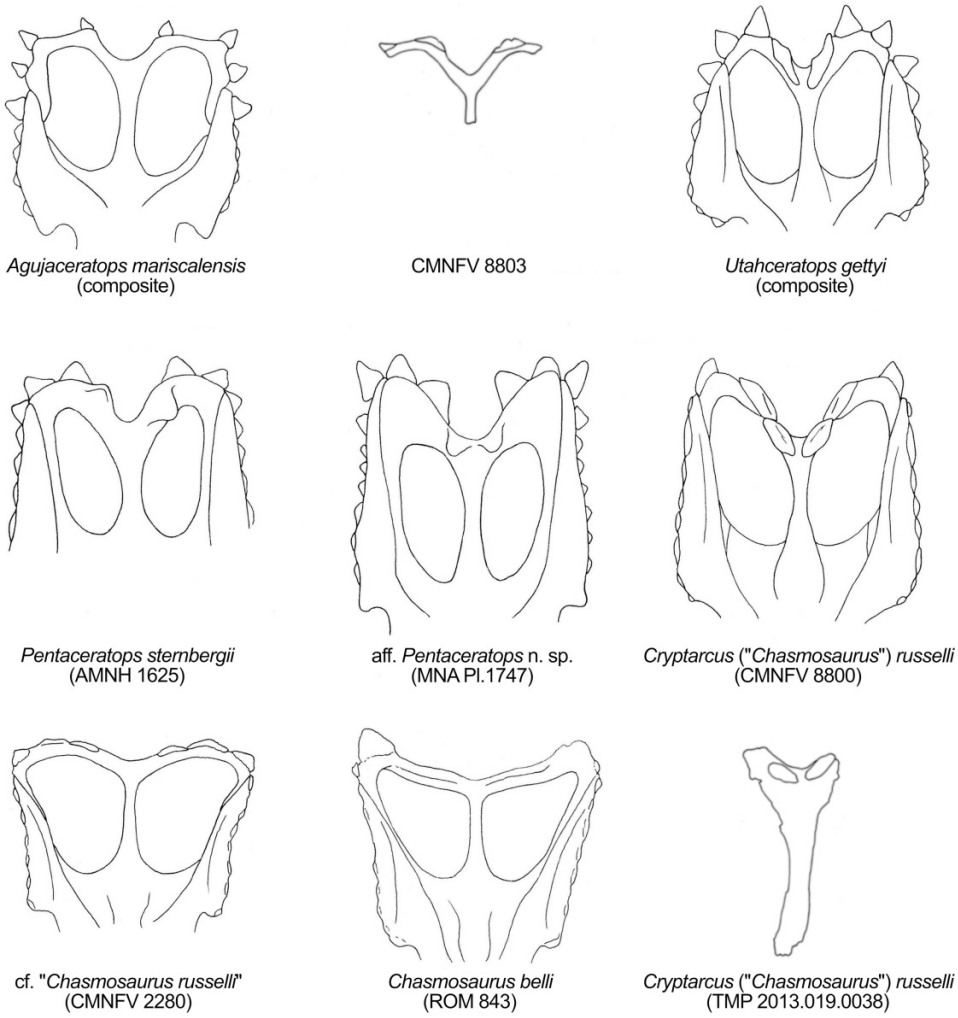

frill. This is unlike *Agujaceratops*, in which the lateral margin is markedly convex in dorsal aspect; as a result, the posterior two-thirds of the bone is distinctly broader than in typical *Chasmosaurus* (Forster et al. 1993). The anterior portion of the squamosal has a quasi-vertical orientation, but flares slightly laterally towards its ventral edge, reaching maximum lateral extent at the third episquamosal (es6) posterior to the jugal notch. Viewed laterally, the anterior-most portion of the dorsal edge of the squamosal turns dorsally, posterior to which it is essentially straight, as in most *Chasmosaurus*. This is in contrast to *Agujaceratops*, in which this dorsal curvature is extended posteriorly, producing a more dorsally concave, upright frill (Forster et al. 1993; Lehman et al. 2017). The ventral surface of the squamosal is inaccessible, but its preserved morphology suggests that, as in all ceratopsids, it formed an elongate, grooved articulation with the quadrate. Dorsally, the squamosal turns medially to form the lateral margin of the supratemporal fenestra but does not contribute to any portion of the floor of the supratemporal fossa. More posteriorly, the squamosal forms approximately one-third of the lateral margin of the parietal fenestra. Its posterior tip terminates slightly anterior to the posterior margin of the frill.

The central portion of the parietal extends anteriorly between the supratemporal fenestrae, where it defines the posterior margin of the frontoparietal fontanelle. Anterolateral to this, it extends a process to the posteromedial corner of each postorbital. The smooth, rounded, dorsal surface of each process forms the floor of a recessed dorsotemporal channel that connects the supratemporal fenestra with the supracranial sinus of the pneumatic diverticulum (Farke 2010). Posterior to this, it forms a gently dome-shaped skull roof that lacks a median crest.

The narrow but stout longitudinal median bar of the parietal is nearly straight, bowing only slightly dorsally. The bar is essentially square in cross section, in sharp contrast with other chasmosaurines (CMNFV 2280 approaches this robust morphology, but the bar is V-shaped in cross section), in which this bar is distinctly wider than deep. Viewed dorsally, its narrowest point is located approximately at its midpoint (Fowler and Freedman Fowler 2020), in contrast with typical

Chasmosaurus, in which the narrowest point is usually near the posterior end of the bar (e.g., Godfrey and Holmes 1995). The preserved left side of the transverse posterior parietal is distinctly bar-like, as in *C. belli* and *Utahceratops*, and does not form an anteroposteriorly broad apron like that seen in *Anchiceratops*, aff. *Pentaceratops* n. sp. (MNA Pl. 1747), *Navajoceratops*, and *Terminocavus* (Fowler and Freedman Fowler 2020). It is dorsoventrally thickest medially where it originates seamlessly from the posterior end of the median bar and thins laterally to a dorsoventral thickness equivalent to 50% of anteroposterior width at its lateral corner. The posterior parietal bar is strongly arched in dorsal aspect to form a deep midline embayment, with the preserved left posterior bar forming an angle of about 35° with the sagittal plane. The posterior margin of the frill of CMNFV 8800 therefore would have formed an M-shaped outline with the posterior-most projecting portion of each arch located near its posterolateral corner. This arching is distinctly more pronounced than in other skulls traditionally attributed to *C. russelli* (e.g., CMNFV 2280, TMP 1981.019.0175, TMP 1983.025.0001). Cambell et al. (2016) conducted a quantitative analysis of frill shape in *Chasmosaurus* and determined that the frill of CMNFV 8800 exhibited the most extreme morphology of all *Chasmosaurus* with respect to morphology of the posterior parietal bar. They nevertheless accepted that this specimen was conspecific with the other specimens attributed to *C. russelli*. Visual comparisons with other chasmosaurines (Fig. 6) suggest similarities with the "*Pentaceratops* clade" taxa such as *Pentaceratops*, *Utahceratops*, and *Agujaceratops*. However, Campbell et al. (2016) did not include any of these taxa in their analysis. Lateral to the inflection point of the arch, the posterior bar turns anteriorly, becoming confluent with the lateral bar. The lateral bar becomes progressively thinner anteriorly and "pinches out" before reaching the midpoint of the parietal fenestra, so does not contact the anterior portion of the lateral bar. Consequently, the medial margin of the squamosal contributes to the lateral margin of the parietal fenestra. A similar morphology is present in other skulls attributed to *C. russelli* (e.g., CMNFV 2280, TMP 1981.019.0175, TMP 1983.025.0001). This morphology has also been described in *Agujaceratops* (Lehman 1989) and illustrated for *Utahceratops* (Sampson et al. 2010, fig. 3).

Frill epiossifications

CMNFV 8800 has been described as having many small episquamosals (Sternberg 1940), perhaps as many as 10 (Campbell et al. 2016), but removal of varnish and further preparation has allowed us to establish a definitive count of eight on the left side. All episquamosals (here abbreviated "es") are low, rounded ossifications that attach to the edge of the squamosal by lenticular bases. Following common usage (e.g., Loewen et al. 2024), epiossifications will be numbered from the posterior to the anterior of the squamosal. With the exception the most anterior epiossification (es8), they all extend thin laminae dorsally to sheath the dorsal surface of the surrounding squamosal. It is unclear whether the episquamosals possess ventral laminae, as the ventral aspect of the squamosal is not exposed. The most anterior episquamosal (es8), which is the smallest (base length of 31 mm), occupies the posteroventral corner of the jugal notch. Dorsomedial to es8, the anterior edge of the squamosal bears a lenticular divot or facet. This may have borne a small supernumerary episquamosal, but no other known chasmosaurine possesses an epiossification in this position. The next six episquamosals become progressively larger (basal lengths of 60, 90, 95, 95, 150, and 205 mm, respectively). The unusually elongate bases of es3 and es2 likely caused prior workers to assume that two or more epiossifications occupied each of their loci, but the well-defined bone grain clearly radiates outward from a single central position on each epiossification, thereby discounting any notion that they represent the coalescence of two smaller epiossifications (Figs. 3E and 3F). The most posterior episquamosal (es1), as preserved, is approximately 50 mm long. However, a weakly defined facet on the edge of the squamosal posterior to this element suggests that a portion might be missing; nevertheless, the complete episquamosal would not have exceeded 120 mm in length, thus reversing the anteroposterior trend of increasing base length exhibited by es8–es2. This pattern has no equivalent in Chasmosaurinae, in which the episquamosals tend to be either subequal in size (e.g., *Chasmosaurus*: CMNFV 2280, ROM 843) or become progressively larger in the posterior direction, with the most posterior epiossification being the largest (e.g., *Pentaceratops*, *Utahceratops*).

There are three epiparietals (here abbreviated "ep") on the preserved left side of the posterior parietal bar contra Sternberg (1940), who reported that epiparietals were absent, likely because of the atypical morphology of ep1 and ep2 (see below), and the incomplete preservation of ep3. In contrast with most chasmosaurines, in which the epiparietals attach to the posterior edge of the posterior bar, the most medial epiparietal (ep1) occupies the dorsal surface of the bar, covering nearly all of its surface adjacent to the midline. It is oval in dorsal outline and dome-shaped with a low longitudinal keel. Its long axis is quasi-parallel with the axis of the bar, forming an angle of 40° with the sagittal. The second epiparietal (ep2), also dome-shaped and broadly keeled, contacts ep1 along a diagonal suture such that, under casual observation, it is hard to distinguish the two ossifications. Its anteromedial end occupies the dorsal surface of the posterior bar, but posterodistally it turns gradually onto the external edge of the bar, so the posterodistal end faces into the median parietal embayment. Immediately lateral to the distal end of ep2, the posterior bar curves laterally. The medial remnant of ep3 is located 90 mm lateral to ep2. Immediately lateral to this remnant, the rounded posterolateral margin of the posterior bar bears a 120 mm long facet, presumably for the remainder of the largely missing ep3, indicating that its base was comparable in length to those of ep1 or ep2. The ep3 locus would have approached, but not straddled, the squamosal-parietal suture. The morphology of this remnant suggests that, in contrast to the robust, dome-shaped morphology of ep1 and ep2, ep3 of CMNFV 8800 was a dorsoventrally flattened, posteriorly projecting plate-like epiossification that lay in the plane of the frill as it does in most chasmosaurines, although whether

it was triangular, boss-shaped, or D-shaped cannot be determined.

Both the morphology and placement of ep1 and ep2 in CMNFV 8800 contrast sharply with that of other specimens previously assigned to *Chasmosaurus russelli*. In the latter skulls (e.g., CMNFV 2280, CMNFV 8803, TMP 1983.025.0001), ep1 is located relatively far from the sagittal plane, and the remaining two epiparietals are spaced more-or-less evenly around the curved posterior margin of the parietal with ep3 located close to the lateral corner of the posterior bar near its articulation with the posterior end of the squamosal (Godfrey and Holmes 1995, figs. 1 and 4). In CMNFV 8800, ep1 is located at the base of the median embayment, nearly touching its bilateral counterpart at the midline. The loci of ep1 and ep2 are contiguous; both are located completely within the embayment. ep3, which is separated from ep2 by a considerable gap, is the only epiparietal that occupies a position comparable to its homologue in other skulls traditionally assigned to *C. russelli*. The placement of the epiossifications in CMNFV 8800 are more comparable to the conditions exhibited in some members of the "*Pentaceratops* clade", in particular *Utahceratops*, aff. *Pentaceratops* n. sp. (MNA Pl. 1747) (but less so *Pentaceratops sternbergii*), *Navajoceratops*, and *Terminocavus* (see Fowler and Freedman Fowler 2020), although in no case is the morphological overlap complete.

Description of TMP 2013.019.0038

This is a partial parietal (Figs. 5A and 5B) consisting of a midline ramus lacking only the anterior-most margin (610 mm preserved midline length), as well as both left and right rami of the posterior bar that extend sufficiently laterally to include the medial-most epiparietals (ep1). Its morphology is closely comparable to that of CMNFV 8800. The expanded anterior portion of the parietal is dome-shaped with a concave ventral surface. Immediately posterior to this, the cross-section of the midline bar is a modified I-beam in shape with a flat ventral surface. At mid-length, the cross-section of the bar transitions into a depressed oval with a flattened ventral surface; posteriorly, the ventral surface becomes gently concave. There are several pronounced grooves on the posteroventral surface. The medial-most groove is the deepest and reaches the ventral edge of the midline, while narrower, more lightly inscribed grooves arc along the right and left preserved portions of the posterior bars. As in CMNFV 8800, the bar in dorsal view is narrowest (70 mm) at approximately mid-length with the posterior portion fanning out to join the broad-based medial portions of the posterior rami. As in both *Pentaceratops* and *Utahceratops*, a thin, shelf-like flange projects from right and left ventrolateral margins of the midline ramus; this flange diminishes and merges with the lateral margin of the ramus at approximately one-third of the distance from the broken anterior face and posteriorly reappears as a narrow flange where the lateral rami diverge from the midline ramus. The right flange is better preserved, although it is broken posteriorly. These flanges, likely representing the preserved margins of the parietal fenestrae, indicate that the fenestra extended almost the entire length of the midline ramus as in *Utahceratops* but differing from the foreshortened fenestrae of *Pentaceratops*. Dorsally, a pair of narrow longitudinal grooves extend the length of the parietal, accentuating the distinction between the flange and median ramus. Posteriorly, at the point where the fenestral margin turns laterally, each groove continues onto the dorsal surface and coalesces with smaller grooves into a larger vascular groove that arches laterally to each ep1 epiparietal. Shorter, less distinct grooves are distributed across the dorsal surface of the parietal, as in other ceratopsids.

Posteriorly, the midline bar is concave dorsally and convex ventrally. As in CMNFV 8800, the posterior parietal margin is U-shaped in dorsal profile. Only the medial stumps of the left and right rami of the posterior bar are preserved, but as in CMNFV 8800 each appears to form an angle of approximately 35° with the sagittal. The preserved portions of the posterior rami (preserved width = 320 mm) are inflated, and the right caudal ramus has several low bumps along its surface. Both ep1 and ep2 are elongate, low, and rounded, and closely resemble those of CMNFV 8800, although they are relatively smaller. They are well fused to the dorsal surface of the bar and positioned sub-parallel to, and inset from, the posterior margin by approximately 10 and 20 mm on the left and right sides, respectively. The dorsally teardrop-shaped right ep1 is approximately 110 mm in length and 70 mm wide medially, with the process tapering to a pointed apex laterally; there is a distinct groove running around its lateral base. At the medioventral base of the right ep1 is a small fossa that may represent a lesion or drainage channel. The left ep1 is ovoid in dorsal view; it is 125 mm in length and is 45 mm in maximum width (at the midpoint). The asymmetrical positioning of the left and right ep1 relative to the midline and the teardrop shape of the right ep1 may be the result of taphonomic distortion that appears to have slightly crushed the element dorsoventrally. At the preserved right posterolateral corner, at the level of ep1, is a small, rostroventrally projecting flange that may represent a portion of an additional medially positioned epiparietal.

Phylogenetic analysis

The results of our cladistic analyses are summarized in Table 3 and Fig. 7. For all iterations, retention indices approach 0.9, indicating good character state retention, and consistency indices approach 0.45, indicating a moderate amount of homoplasy (presumably, due to convergence). Bootstrap support values are moderate, at best, and weak across most of the tree. In the first two iterations, we were unable to resolve CMNFV 8800 as closer to either *Chasmosaurus* or *Pentaceratops*. In two of the remaining four iterations, CMNFV 8800 either pairs with the (*Chasmosaurus*, "*Mojoceratops*") clade or else is recovered as closer to the (*Agujaceratops*, (*Navajoceratops*, (*Utahceratops*, *Pentaceratops*))) clade. We were unable to replicate the topology of Loewen et al. (2024) in which CMNFV 8800 falls closer to the (*Pentaceratops*, *Utahceratops*) group than does *Agujaceratops*, although the monophyly of the latter is not consistently recovered across our consensus trees.

In the two strict consensus trees uniting CMNFV 8800 with the (*Chasmosaurus*, "*Mojoceratops*") clade, the single recovered synapomorphy is character 82: 0→1 (facial skeleton in region

Table 3. Summary of iterative cladistic analysis.

Iteration	No. of MPTs	Best score (fit)	CI	RI	Strict consensus topology
1	1579	922	0.454	0.892	CMNFV 8800, (‘*Mojoceratops*’, *Chasmosaurus*), (*Navajoceratops*, (*Agujaceratops*, (*Pentaceratops*, *Utahceratops*)))
2	575	936	0.454	0.892	CMNFV 8800, (‘*Mojoceratops*’, *Chasmosaurus*), (*Navajoceratops*, (*Agujaceratops*, (*Pentaceratops*, *Utahceratops*)))
3	14	986 (85.706)	0.449	0.890	CMNFV 8800, *Agujaceratops*, (*Navajoceratops*, (*Pentaceratops*, *Utahceratops*))
4	7	980 (32.760)	0.452	0.891	CMNFV 8800, (‘*Mojoceratops*’, *Chasmosaurus*)
5	14	986 (85.706)	0.449	0.890	CMNFV 8800, *Agujaceratops*, (*Navajoceratops*, (*Pentaceratops*, *Utahceratops*))
6	7	980 (32.760)	0.452	0.891	CMNFV 8800, (‘*Mojoceratops*’, *Chasmosaurus*)

Note: See also Fig. 7. Abbreviations: CI, consistency index; MPTs, most parsimonious trees; RI, retention index.

of orbits shallow, maxilla dorsoventrally low, posterior ramus of maxilla partially covered by jugal). In the two strict consensus trees in which CMNFV 8800 plots closer to *Pentaceratops* than to *Chasmosaurus*, the three synapomorphies uniting this more inclusive clade are: character 108: 0→1 (jugal infratemporal process short), character 149: 0→2 (concave median embayment on posterior edge of parietal restricted to center margin, deep, notch-like), and character 183:1→0 (fossa present on posterior surface of basal tubera), although it should be noted that only character 149 can be coded for CMNFV 8800. Using the “move branch” tool in Mesquite v. 3.81 (Maddison and Maddison 2023), alternatively positioning CMNFV 8800 as closer to *Chasmosaurus* or *Pentaceratops* changes the length of the tree by one (iterations 4 and 6) or three steps (iterations 3 and 5).

Discussion

Taxonomic justification

We are keenly aware that the historical ceratopsian literature is rife with taxonomic names based on material of dubious diagnostic value. We do not wish to compound the problem. However, our re-examination of CMNFV 8800 has made it apparent, as has been suggested previously (e.g., Fowler and Freedman Fowler 2020; Barrera Guevara et al. 2024; Loewen et al. 2024), that neither it nor the closely comparable partial parietal (TMP 2013.019.0038) more recently collected from the Onefour area can be accommodated within *Chasmosaurus* or, for that matter, any other known chasmosaurine genus. As such, we argue that it is necessary to remove CMNFV 8800 from *Chasmosaurus* and erect a new genus, *Cryptarcus*, to receive it.

Sternberg (1940) did not explicitly provide his reasoning for attributing CMNFV 8800 to *Chasmosaurus*, but he was clearly impressed by the long and low face, the apparent reduction of the postorbital horncores, and the strut-like parietal, all to which he drew attention in his original description. However, in the 85 years since Sternberg published his description, many new chasmosaurines have been discovered (Dodson 2013), and the mosaic distribution of these characters within Chasmosaurinae has become more apparent. The low facial profile of CMNFV 8800 occurs in several other chasmosaurine taxa, including at least one specimen of *Anchiceratops* (CMNFV 8535), *Agujaceratops mavericus* Lehman, Wick, and Barnes 2017, and *Pentaceratops*. In two of the six iterations of our cladistic analysis that pair CMNFV 8800 with the clade (*C. belli*, “*Mojoceratops perifania*”), the single synapomorphy uniting them is Character 82:0→1 (dorsoventral depth of facial skeleton shallow, maxilla dorsoventrally low, posterior ramus of maxilla partially covered by jugal). However, as revealed by Mallon et al. (2011), this character is subject to taphonomic distortion and is intraspecifically variable in at least *Anchiceratops ornatus*. If polymorphisms are appropriately coded in matrix from Loewen et al. (2024) that we modified for this study (which is a gargantuan task beyond the scope of this study), the alliance between CMNFV 8800 and *Chasmosaurus* would be correspondingly reduced.

A parietal composed of thin, strut-like median and transverse bars enclosing enlarged fenestrae is also more broadly distributed among chasmosaurines than originally appreciated by Sternberg (1940); it is also found in *Agujaceratops* and *Utahceratops*. The former was, in fact, originally assigned to *Chasmosaurus*, based largely on the presence of this parietal structure (Lehman 1989). However, subsequent cladistic analyses have repeatedly recovered it as closer to *Pentaceratops* (Sampson et al. 2010; Loewen et al. 2024), necessitating the coining of a new genus.

While Sternberg (1940, p. 479) remarked on the perceived lack of a postorbital horncore in “*C.*” *russelli* (or, at most, “there may have been a short horn”), resembling the condition in most *C. belli*, our re-examination of the holotype skull reveals that enlarged horncores were likely once present. To be sure, long postorbital horncores are also present in some specimens traditionally assigned to *Chasmosaurus* (i.e., *C.* “*canadensis*”; *C.* “*kaiseni*”; “*Mojoceratops perifania*”, all considered by most workers to be a junior synonym of *C. russelli* sensu lato (Maidment and Barrett 2011; Konishi 2015; Campbell et al. 2016)), but they are also widespread throughout Ceratopsidae, being primitive for the clade (Longrich 2010). The likely presence of elongate horncores in CMNFV 8800 is therefore of limited diagnostic value.

Referencing the most recent diagnosis of *Chasmosaurus* (Campbell et al. 2016), which includes the specimens from

Fig. 7. Strict consensus trees produced by iterative cladistic analysis. (A) topology recovered by iterations 1, 2, 4, and 6; (B) topology recovered by iterations 3 and 5. Bootstrap support ≥50% indicated above nodes.

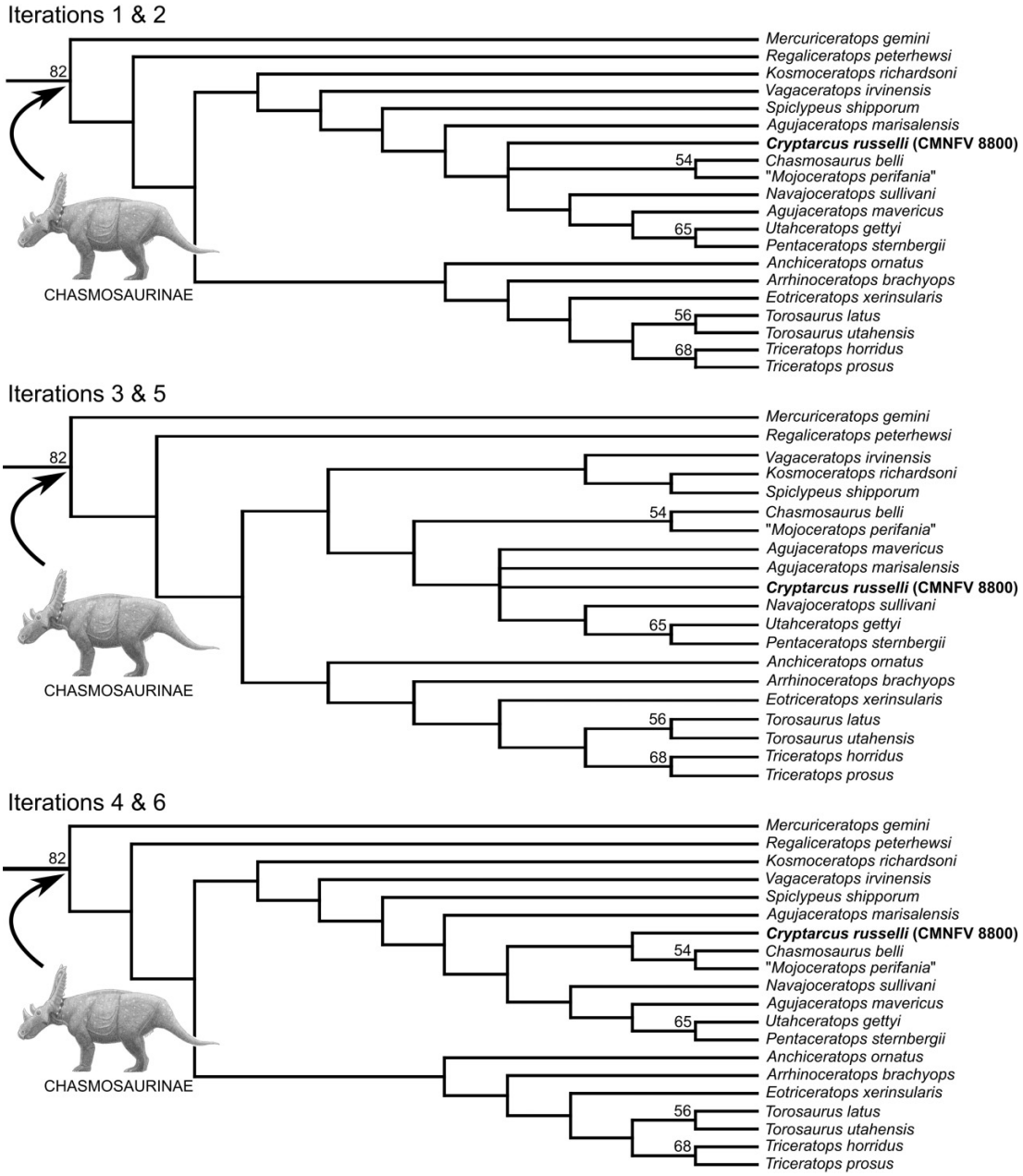

the lower Dinosaur Park Formation traditionally included in the hypodigm of *C. russelli*, we draw attention to several other points of disagreement with CMNFV 8800, which have come to light since our own examination of the skull. Campbell et al. (2016, p. 34) diagnosed the genus as follows:

> *Chasmosaurus* is diagnosed based on the following unique combination of characters: (1) Premaxillary flange along entire anterior margin of external naris; (2) postorbital horncores, when present, curve posteriorly along their length; (3) squamosal dorsal border laterally adjacent to dorsal temporal fenestra straight in profile, anteriorly at level with base of postorbital horncore, and sloping posteroventrally at a shallow angle before ascending farther posteriorly to form lateral border of parietal fenestra; (4) medial margin of squamosal, where it articulates with the lateral bar of the parietal, straight; (5) frill broadens posteriorly to form rectangular to triangular shield with maximum width more than twice the skull width at orbits; (6) parietal fenestrae large, occupying most of the parietal, and being rounded or anteroposteriorly longer than transversely wide; and (7) epiparietals straight and triangular in shape and oriented posteriorly or anterodorsally.

Traits (2) and (6) were addressed above. The presence of trait (1) cannot be determined in CMNFV 8800 due to poor preservation of this region. Trait (3) is not restricted to *Chasmosaurus*, occurring as it does in *Arrhinoceratops brachyops* Parks, 1925 (Mallon et al. 2014), *Regaliceratops peterhewsi* Brown and Hen-

derson 2015, and *Pentaceratops sternbergii* (Osborn 1923), for example. Trait (4) is likewise not unique to *Chasmosaurus* and occurs in several other taxa, including *Utahceratops* (Sampson et al. 2010) and *P. sternbergii* (Osborn 1923). As we have shown here, trait (5) does not, in fact, apply to CMNFV 8800, as the frill, in dorsal projection, is wider anteriorly than posteriorly. Finally, it is inaccurate to describe the epiparietals of CMNFV 8800 as "triangular" (trait 7), as epiparietals ep1 and ep2 in CMNFV 8800 are lenticular in outline and dome shaped. The configuration of the epiparietals and episquamosals differ in several other important ways from typical *Chasmosaurus*, as we describe above. Thus, even the most recent diagnosis of *Chasmosaurus* applies poorly to CMNFV 8800.

If CMNFV 8800 cannot be assigned to *Chasmosaurus*, where do its affinities lie? Recent assessments have placed it closer to *Pentaceratops*, either as part of an anagenetic sequence leading to *Terminocavus* (Barrera Guevara et al. 2024) or else as the sister taxon to either *Coahuilaceratops magnacuerna* or (*Utahceratops*, *Pentaceratops*) (Loewen et al. 2024). Our own results are somewhat more nebulous. In those cladistic iterations (using implied weighting) placing CMNFV 8800 closer to *Pentaceratops* than to *Chasmosaurus*, the topology is otherwise poorly resolved (Fig. 7). CMNFV 8800 is recovered in a polytomy with *Agujaceratops mariscalensis*, *Agujaceratops mavericus*, and (*Navajoceratops*, (*Utahceratops*, *Pentaceratops*)).

We are thus left with a taxonomic conundrum: If CMNFV 8800 does not pertain to *Chasmosaurus*, and if its phylogenetic placement cannot otherwise be resolved within Chasmosaurinae, what should it be called? One option would be to retain the name "*Chasmosaurus*" *russelli*, using scare quotes to denote our uncertainty regarding the generic designation. However, this solution could be misunderstood as suggesting that it is more closely related to *Chasmosaurus* than to the "*Pentaceratops* clade", an implication that is not entirely supported by our results. We instead prefer to erect a new genus—*Cryptarcus*—to receive CMNFV 8800, an approach that recognizes the unique morphology of this specimen without committing to a particular interpretation regarding its phylogenetic status. Further work may yet resolve the species with, e.g., *Agujaceratops*, *Utahceratops*, or *Coahuilaceratops*. If and when this occurs, it can be reassigned to the appropriate genus.

Aggravating factors

Quite aside from the spectre of convergent evolution, there are several difficulties inherent in the evaluation of hypothesized relationships between CMNFV 8800 and the "*Pentaceratops* clade" or, indeed, chasmosaurines more generally. The first concerns insufficient anatomical data, as most members of the "*Pentaceratops* clade" are represented by comparatively incomplete material. As such, many aspects of their anatomy can be only approximated. For example, determination of exact proportions, such as relative widths of the anterior and posterior portions of the frill, is difficult when matching surfaces between fragments are lacking. Furthermore, while the skull reconstructions of *Utahceratops* (Sampson et al. 2010; figs. 3 and 4) are convincing, it must be remembered that much of the original skull material is disarticulated within the context of a bonebed. Therefore, some character codings with respect to the skull proportions of Loewen et al. (2024), as well as character codings in all preceding iterations of their matrix, are necessarily based on composite skull reconstruction(s) rather than the original disarticulated material and should be accepted only provisionally. Similar caution should be extended to character codings in several other ceratopsid taxa derived only from bonebeds, including *Agujaceratops mariscalensis*, in which the holotype locality contains a range of ontogenetic stages (Lehman 1989). To complicate matters further, a nearly complete articulated skull (Forster et al. 1993), which has been used to characterize this taxon in many analyses, may not, in fact, be conspecific (Lehman et al. 2017).

A second complicating factor concerns bilateral asymmetry. Ceratopsid skulls are notoriously prone to asymmetry, owing to both taphonomic distortion and the extended growth trajectory inherent in their natural development (e.g., Lambe 1910; Godfrey and Holmes 1995; Currie et al. 2008; Holmes et al. 2020; Loewen et al. 2024). Relevant to present concerns, one of the few reasonably complete, well-preserved frills attributed to *P. sternbergii* (AMNH 1625) has highly asymmetrical episossifications (Fig. 6); whereas the left ep1 epiparietal curls anterodorsally, the right counterpart projects directly dorsally, rendering the "normal" orientation of ep1 in *P. sternbergii* unclear. Similarly, in one of the most complete parietals of *Utahceratops* (UMNH 16671), the medial-most epiparietals appear to vary in number across the midline; whereas the left side of the element bears two distinct epiparietals within the parietal emargination, the right side has only one. This was not acknowledged in the original description (Sampson et al. 2010), although all subsequent character codings for this taxon appear to reflect the condition exhibited on the right side of the skull. It is potentially possible to derive the "normal" condition with the benefit of additional material, thereby allowing for the calculation of an arithmetic mean, but this is presently not possible given the incompleteness of the fossil record.

A third factor, related to the previous, is intraspecific variation. Ceratopsids not only exhibit asymmetrical skulls, but also a high degree of polymorphism within their populations. Some of this variation may be related to sexual dimorphism (Saitta et al. 2020; Motani 2021; Pintor et al. 2023), but a great deal of it is not (Mallon 2017). This is, perhaps, nowhere better demonstrated than in the Pipestone Creek bonebed containing the scattered bones of *Pachyrhinosaurus lakustai* Currie, Langston, and Tanke 2008, in which individuals of similar size can vary in the convexity of the nasal boss, the number of humps on the median parietal bar, the presence of adventitious hornlets around the principal median parietal horn, and the presence of ep2 hooks (Currie et al. 2008). The tendency toward such ubiquitous intraspecific variation not only complicates character coding but also establishes an expectation that polymorphism should be seen, possibly blinding researchers to the possibility that their working hypodigm contains multiple, subtly different species. Of course, as we argue here, this is precisely the case with the historical hypodigm of *Chasmosaurus russelli*, dating back to its initial description (Sternberg 1940). It is only with the benefit of additional bios-

tratigraphic information that we have come to recognize this longstanding oversight.

None of the foregoing deals with the further complicating and entangled issues of ceratopsid ontogeny (e.g., Sampson et al. 1997; Mallon et al. 2015; Currie et al. 2016; Horner and Goodwin 2006) or competing epiossification homology schemes (Brown and Henderson 2015; Loewen et al. 2024) which have been ably discussed elsewhere and remain at issue. Frustrations similar to the above have appeared in the literature before (e.g., Lehman et al. 2017), but they bear repeating here, with an eye to resolving them.

Implications for the evolution of Chasmosaurinae

The subject of anagenesis as an important mode of evolution among Late Cretaceous dinosaurs has garnered much interest (e.g., Horner et al. 1992; Scannella et al. 2014; Freedman Fowler and Horner 2015; Carr et al. 2017; Mallon et al. 2025). Barrera Guevara et al. (2024) recently hypothesized that CMNFV 8800 formed the beginning of an anagenetic evolutionary sequence, as follows: CMNFV 8800 → *Utahceratops* → *Pentaceratops* → *Navajoceratops* → *Terminocavus*. This hypothesized scenario has its origin in the earlier work of Fowler and Freedman Fowler (2020), who did not initially consider CMNFV 8800 as part of the sequence. Although Barrera Guevara et al. (2024) provided no cladistic analysis in support of their anagenesis hypothesis, Fowler and Freedman Fowler (2020) did. Importantly, in the three cladograms they produced, none were consistent with their hypothesized anagenetic sequence in showing the following predicted nested sets of relationships: "*Chasmosaurus*" *russelli*, (*Utahceratops* (*Pentaceratops*, (*Navajoceratops*, *Terminocavus*))). The authors acknowledged this, suggesting it might be related to the way *Pentaceratops* was coded in their dataset.

Our findings are similarly unsupportive of this anagenetic scenario. In our varied cladistic iterations (Fig. 7), *Utahceratops* is consistently closer to *Pentaceratops* than *Navajoceratops* (*Terminocavus* is coded as part of *Pentaceratops*), and *Agujaceratops mavericus* variably nests closer to (*Pentaceratops*, *Utahceratops*) than does *Navajoceratops*.

Further complications to the anagenetic scenario are introduced by the recent U–Pb dating of Campanian-aged Western Interior strata by Ramezani et al. (2022). Unlike the stratigraphic relationships illustrated by Fowler and Freedman Fowler (2020), Ramezani et al. (2022) found the top of the Dinosaur Park Formation (host to *Cryptarcus russelli*) at Dinosaur Provincial Park, Alberta to be younger than the middle unit of the Kaiparowits Formation in Utah (host to *Utahceratops*). Thus, if these dates are correct, the temporal distributions of *Utahceratops* and *Cr. russelli* are out of sequence with their proposed anagenetic relationship.

It is important to reiterate that, although CMNFV 8800 is roughly coeval with "*Pentaceratops* clade" taxa, in particular *Utahceratops* (Ramezani et al. 2022), it was collected in present-day southern Alberta, far from the known geographic range of the "*Pentaceratops* clade" taxa in the southwestern US. If ceratopsids inhabiting Laramidia during the late Campanian exhibit latitudinal endemism—as suggested by Lehman (1997), Gates et al. (2010, 2023), Loewen et al. (2024), and Barrera Guevara et al. (2024), among others—then the discovery of a close relative of any of these southern taxa in southern Alberta can only be considered anomalous. A similar argument could be made concerning *Vagaceratops* [= *Chasmosaurus*] *irvinensis*] also from southern Alberta. Sampson et al. (2010) argued that it is most closely related to *Kosmoceratops richardsoni* from what is now southern Utah, approximately 1300 km to the south) rather than to the much more proximate *Chasmosaurus* from what is now Dinosaur Provincial Park. More detailed phylogenetic and historical biogeographic analyses are required to address the nature of chasmosaurine faunal interchange between north and south Laramidia.

If the Laramidian ceratopsids did indeed exhibit endemism, we are forced to entertain an alternate scenario to explain the features shared by CMNFV 8800 and the southern ceratopsid taxa. It has been suggested that frill morphology played a role in species recognition and/or sexual selection in ceratopsids (e.g., Farlow and Dodson 1975; Padian and Horner 2011; Hone and Naish 2013; Knapp et al. 2018). If the "*Pentaceratops* clade" taxa were indeed restricted to what is now the southwestern US, an unrelated chasmosaurine living in what is now Alberta would have been free to evolve frill features considered to be diagnostic of one or more of the southern chasmosaurines without risk of accidental misidentification and unproductive interspecific mating. A similar argument has been advanced to account for the surprising occurrence of centrosaurine-like frill features in the chasmosaurine *Regaliceratops* (Brown and Henderson 2015). Such a scenario is quite plausible given the highly modular and plastic nature of the ceratopsian frill (Prieto-Márquez et al. 2020). Future discovery of phylogenetically informative characters of the braincase and palate, regions of the ceratopsid skull that remain poorly known, may resolve the phylogenetic placement of *Cryptarcus*.

Conclusions

The morphology of the holotype of "*Chasmosaurus*" *russelli* (CMNFV 8800) is distinct from that exhibited by all other ceratopsids from the Dinosaur Park Formation, including those specimens that in the past have been referred to this taxon. As such, the latter specimens should be removed from the hypodigm, and only the holotype should be used to diagnose this species. Our iterative cladistic analysis, based on an updated character list of Loewen et al. (2024), variably recovers CMNFV 8800 as either the sister taxon to (*Chasmosaurus*, "*Mojoceratops*") or embedded within the "*Pentaceratops* clade" (Fig. 7). Our present inability to consistently resolve the relationships of CMNFV 8800 within Chasmosaurinae may be due to a variety of intertwined issues, including fossil incompleteness, coding from composite specimens, and the spectre of "intraspecific variation," among others. Although traditionally included within the genus *Chasmosaurus*, CMNFV 8800 exhibits a mosaic of features that are shared by one or more of *Agujaceratops*, *Utahceratops*, *Pentaceratops* and "aff. *Pentaceratops* n. sp." (MNA Pl. 1747). The apparently random distribution of such features among these taxa also likely contributed to our failure to demonstrate a specific relationship between

CMNFV 8800 and any of these taxa. As such, there is no basis of support for assignment of CMNFV 8800 to any of these established genera, although additional data may change this in the future. Nevertheless, CMNFV 8800 is both clearly diagnosable and clearly distinguishable from any other known chasmosaurine. Therefore, we erect the genus *Cryptarcus* to accommodate the holotype of "*Chasmosaurus*" *russelli*. We will deal with those other specimens from the lower Dinosaur Park Formation traditionally assigned to "*C.*" *russelli* in a future contribution.

Acknowledgements

We thank M. Loewen and A. Farke for answering questions relating to the data matrix of Loewen et al. (2024) and for providing helpful reviews. Valuable information and opinion related to chasmosaurine phylogenetics was also provided by R. Mansergh. Thanks also to C. Sullivan for shepherding the manuscript through the editorial process. We appreciate K. Myhran for bringing a subtle but crucial error to our attention at the last minute of publication. Fine preparation of CMNFV 8800 was provided S. Pan. TMP 2013.019.0038 was collected by the 2013 Southern Alberta Dinosaur Project under OPAC permits to collect palaeontological resources #13-013 (DCE) and 13-022 (MJR). The TNT software used for our phylogenetic analysis was made freely available by the Willi Hennig Society.

Article information

History dates

Received: 5 April 2025
Accepted: 24 November 2025
Version of record online: 25 March 2026

Copyright

Author information

Author ORCIDs

Robert B. Holmes https://orcid.org/0009-0000-9220-2950
Jordan C. Mallon https://orcid.org/0000-0002-8209-8827
Michael J. Ryan https://orcid.org/0000-0001-6039-3748

Author contributions

Conceptualization: RBH, JCM, MJR, DCE
Data curation: JCM
Formal analysis: RBH, JCM, MJR
Funding acquisition: DCE, JCM, MJR
Investigation: RBH, JCM, MJR, DCE
Methodology: RBH, JCM
Project administration: RBH
Resources: JCM, MJR
Software: JCM
Visualization: RBH, JCM, MJR
Writing – original draft: RBH, JCM
Writing – review & editing: RBH, JCM, MJR, DCE

Competing interests

The authors have no competing interests to declare.

Funding information

JCM is supported by researching funding from the Canadian Museum of Nature.
Fieldwork associated with this project was conducted as part of the Southern Alberta Dinosaur Project (SADP); Funding for some students participating in the SADP was provided, in part, by the Dinosaur Research Institute and the Royal Ontario Museum. DCE was supported by an NSERC Discovery Grant (NSERC Grant File Number: RGPIN-2018-06788), and stratigraphic fieldwork in 2025 was supported by Royal Ontario Museum Peer Review Research Grant.

Supplementary material

Supplementary data are available with the article at https://doi.org/10.1139/cjes-2025-0031.

References

Barrera Guevara, D., Espinosa Chávez, B., Serrano Brañas, C.I., de León Davila, C., Postida Martinez, D., Freedman Fowler, E., and Fowler, D. 2024. Stratigraphic reassessment of the Mexican chasmosaurine *Coahuilaceratops magnacuerna* as the first diagnostic dinosaur remains from the Cerro Huerta Formation (lower Maastrichtian) supporting the southern origin of the Triceratopsini. Diversity, **16**: 1–12. doi:10.3390/d16070390.

Brown, B. 1914. *Anchiceratops*, a new genus of horned dinosaurs from the Edmonton Cretaceous of Alberta. With a discussion of the origin of the ceratopsian crest and the brain casts of *Anchiceratops* and *Trachodon*. Bulletin of the American Museum of Natural History, **33**: 539–548.

Brown, B. 1933. A new longhorned Belly River ceratopsian. American Museum Novitates, **649**: 1–9.

Brown, C.M., and Henderson, D.M. 2015. A new horned dinosaur reveals convergent evolution in cranial ornamentation in Ceratopsidae. Current Biology, **25**: 1641–1648. doi:10.1016/j.cub.2015.04.041.

Brown, C.M., Russell, A.P., and Ryan, M.J. 2009. Pattern and transition of surficial bone texture or the centrosaurine frill and their ontogenetic and taxonomic implications. Journal of Vertebrate Paleontology, **29**: 132–141. doi:10.1671/039.029.0119.

Campbell, J.A., Ryan, M.J., Holmes, R.B., and Schröder-Adams, C.J. 2016. A re-evaluation of the chasmosaurine ceratopsid genus *Chasmosaurus* (Dinosauria: Ornithischia) from the Upper Cretaceous (Campanian) Dinosaur Park Formation of Western Canada. PLoS ONE, 1–39. doi:10.1371/journal.pone.0145805.

Carr, T.D., Varricchio, D.J., Sedlmayr, J.C., Roberts, E.M., and Moore, J.R. 2017. A new tyrannosaur with evidence for anagenesis and crocodile-like facial sensory system. Scientific Reports, **7**(1): 44942. doi:10.1038/srep44942.

Currie, P.J., Holmes, R.B., Ryan, M.J., and Coy, C. 2016. A juvenile chasmosaurine ceratopsid (Dinosauria, Ornithischia) from the Dinosaur Park Formation, Alberta, Canada. Journal of Vertebrate Paleontology, **36**: e1048348. doi:10.1080/02724634.2015.1048348.

Currie, P.J., Langston, W., Jr., and Tanke, D.H. 2008. A new species of *Pachyrhinosaurus* (Dinosauria, Ceratopsidae) from the Upper Cretaceous of Alberta, Canada. *In* A New Horned Dinosaur from an Upper Cretaceous Bone Bed in Alberta. *Edited by* P.J. Currie, W. Langston, Jr. and D.H. Tanke. NRC Research Press, Ottawa. p. 1–108. doi:10.1139/9780660198194.

Dodson, P. 2013. Ceratopsia increase: history and trends. Canadian Journal of Earth Sciences, **50**: 294–305. doi:10.1139/cjes-2012-0085.

Eberth, D.A. 1996. Origin and significance of mud-filled incised valleys (Upper Cretaceous) in southern Alberta, Canada. Sedimentology, **43**: 459–477. doi:10.1046/j.1365-3091.1996.d01-15.x.

Eberth, D.A. 2024. Stratigraphic architecture of the Belly River Group (Campanian, Cretaceous) in the plains of southern Alberta: revisions and updates to an existing model and implications for correlating dinosaur-rich strata. PLoS ONE, **19**(1): e0292318. doi:10.1371/journal.pone.0292318.

Eberth, D.A., and Brinkman, D.B. 1997. Paleoecology of an estuarian, incised-valley fill in the Dinosaur Park Formation (Judith River Group, Upper Cretaceous) of southern Alberta, Canada. Palaios, **12**: 43–58. doi:10.2307/3515293.

Eberth, D.A., Evans, D.C., Ramezani, J., Kamo, S.L., Brown, C.M., Currie, P.J., and Braman, D.R. 2023. Calibrating geologic strata, dinosaurs and other fossils at Dinosaur Provincial Park (Alberta, Canada) using a new CA-ID-TIMS U-Pb geochronology. Canadian Journal of Earth Sciences, **60**(12): 1627–1646. doi:10.1139/cjes-2023-0037.

Farke, A.A. 2010. Evolution, homology, and function of the supracranial sinuses in ceratopsian dinosaurs. Journal of Vertebrate Paleontology, **30**: 1486–1500. doi:10.1080/02724634.2010.501436.

Farlow, J.O., and Dodson, P. 1975. The behavioral significance of frill and horn morphology in ceratopsian dinosaurs. Evolution, **29**: 353–361. doi:10.1111/j.1558-5646.1975.tb00214.x.

Forster, C.A. 1996. New information on the skull of *Triceratops*. Journal of Vertebrate Paleontology, **16**: 246–258. doi:10.1080/02724634.1996.10011312.

Forster, C.A., Sereno, P.C., Evans, T.W., and Rowe, T. 1993. A complete skull of *Chasmosaurus mariscalensis* (Dinosauria: Ceratopsidae) from the Aguja Formation (late Campanian) of West Texas. Journal of Vertebrate Paleontology, **13**: 161–170. doi:10.1080/02724634.1993.10011498.

Fowler, D.W., and Freedman Fowler, E.A. 2020. Transitional evolutionary forms in chasmosaurine ceratopsid dinosaurs: evidence from the Campanian of New Mexico. PeerJ, **8**: e9251. doi:10.7717/peerj.9251.

Fredrickson, J.A., and Tumarkin-Deratzian, A.R. 2014. Craniofacial ontogeny in *Centrosaurus apertus*. PeerJ, **2**: e252. doi:10.7717/peerj.252.

Freedman Fowler, E.A., and Horner, J.R. 2015. A new brachylophosaurin hadrosaur (Dinosauria: Ornithischia) with an intermediate nasal crest from the Campanian Judith River Formation of Northcentral Montana. PLoS ONE, **10**: e0141304. doi:10.1371/journal.pone.0141304.

Galton, P.M. 1974. The ornithischian dinosaur *Hypsilophodon* from the Wealdon of the Isle of Wight. Bulletin of the British Museum (Natural History) Geology, **25**: 1–152. doi:10.5962/p.313819.

Gates, T.A., Cai, H., Hu, Y., Han, X., Griffith, E., Burgener, L., et al. 2023. Estimating ancient biogeographic patterns with statistical model discrimination. The Anatomical Record, **306**: 1880–1895. doi:10.1002/ar.25067.

Gates, T.A., Sampson, S.D., Zanno, L.E., Roberts, E.M., Eaton, J.G., Nydam, R.L., et al. 2010. Biogeography of terrestrial and freshwater vertebrates from the Late Cretaceous (Campanian) Western Interior of North America. Palaeogeography, Palaeoclimatology, Palaeoecology, **291**: 371–387. doi:10.1016/j.palaeo.2010.03.008.

Godfrey, S.J., and Holmes, R. 1995. Cranial morphology and systematics of *Chasmosaurus* (Dinosauria: Ceratopsidae) from the Upper Cretaceous of Western Canada. Journal of Vertebrate Paleontology, **15**: 726–742. doi:10.1080/02724634.1995.10011258.

Goloboff, P.A. 2014. Extended implied weighting. Cladistics, **30**(3): 260–272. doi:10.1111/cla.12047.

Goloboff, P.A., and Catalano, S.A. 2016. TNT version 1.5, including a full implementation of phylogenetic morphometrics. Cladistics, **32**: 221–238. doi:10.1111/cla.12160.

Goloboff, P.A., Torres, A., and Arias, J.S. 2018. Weighted parsimony outperforms other methods of phylogenetic inference under models appropriate for morphology. Cladistics, **34**: 407–437. doi:10.1111/cla.12205.

Holmes, R.B, Persons, W.S., Rupal, B.S., Qureshi, A.J., and Currie, P.J. 2020. Morphological variation and asymmetrical development in the skull of *Styracosaurus albertensis*. Cretaceous Research, **107**: 104308. doi:10.1016/j.cretres.2019.104308.

Holmes, R.B., Forster, C.A., Ryan, M.J., and Shepherd, K.M. 2001. A new species of *Chasmosaurus* (Dinosauria: Ceratopsidae) from the Dinosaur Park Formation of southern Alberta. Canadian Journal of Earth Sciences, **38**: 1423–1438. doi:10.1139/e01-036.

Hone, D.W., and Naish, D. 2013. The 'species recognition hypothesis' does not explain the presence and evolution of exaggerated structures in non-avialan dinosaurs. Journal of Zoology, **290**: 172–180. doi:10.1111/jzo.12035.

Horner, J.R., and Goodwin, M.B. 2006. Major changes during Triceratops ontogeny. Proceedings of the Royal Society B, **273**: 2757–2761. doi:10.1098/rspb.2006.3643.

Horner, J.R., Varricchio, D.J., and Goodwin, M.B. 1992. Marine transgressions and evolution of Cretaceous dinosaurs. Nature, **358**: 59–61.

Kirkland, J.I., and Deblieux, D.D. 2010. New basal centrosaurine ceratopsian skulls from the Wahweap Formation (middle Campanian), Grand Staircase-Escalante National Monument, southern Utah. *In* New perspectives on horned dinosaurs: the royal tyrrell museum ceratopsian symposium. *Edited by* M.J. Ryan, B.J. Chinnery-Allgeier and D.A. Eberth. Indiana University Press, Bloomington, Indiana. p. 117–140.

Knapp, A., Knell, R.J., Farke, A.A., Loewen, M.A., and Hone, M.A. 2018. Pattern of divergence in the morphology of ceratopsian dinosaurs: sympatry is not a driver of ornament evolution. Proceedings of the Royal Society of London B, **285**: 20180312. doi:10.1098/rspb.2018.0312.

Konishi, T. 2015. Redescription of UALVP 40, an unusual specimen of *Chasmosaurus* Lambe 1914 (Ceratopsidae: Chasmosaurinae) bearing long postorbital horns, and its implications for ontogeny and alpha taxonomy of the genus. Canadian Journal of Earth Sciences, **52**: 608–619. doi:10.1139/cjes-2014-0167.

Lambe, L.M. 1902. On Vertebrata of the mid-Cretaceous of the North West territory. 2. New genera and species from the Belly River Series (mid-Cretaceous). Geological Survey of Canada Contributions to Palaeontology, **3**: 25–81.

Lambe, L.M. 1910. Note on the parietal crest of *Centrosaurus* and a proposed new generic name for *Stereocephalus tutus*. Ottawa Naturalist, **24**: 149–151.

Lambe, L.M. 1914. On *Gryposaurus notabilis*, a new genus and species of trachodont dinosaur from the Belly River Formation of Alberta, with a description of the skull of *Chasmosaurus belli*. Ottawa Naturalist, **27**: 145–155.

Lehman, T.M. 1989. *Chasmosaurus mariscalensis*, sp. nov., a new ceratopsian dinosaur from Texas. Journal of Vertebrate Paleontology, **9**: 137–162. doi:10.1080/02724634.1989.10011749.

Lehman, T.M. 1990. The ceratopsian subfamily Chasmosaurinae: sexual dimorphism and systematics. *In* Dinosaur systematics. *Edited by* K. Carpenter and P.J. Currie. Cambridge University Press, Cambridge, UK. p. 211–230. doi:10.1017/CBO9780511608377.

Lehman, T.M. 1996. A horned dinosaur from the El Picacho Formation of West Texas, and review of ceratopsian dinosaurs from the American Midwest. Journal of Paleontology, **70**: 494–508. doi:10.1017/S0022336000038427.

Lehman, T.M. 1997. Late Campanian dinosaur biogeography in the Western Interior Seaway of North America. *In* Dinofest International: Proceedings of a Symposium held at Arizona State University. *Edited by* D.L. Wolberg, E. Stump and G.D. Rosenberg. Academy of Natural Sciences, Philadelphia. p. 223–240.

Lehman, T.M. 1998. A gigantic skull and skeleton of the horned dinosaur *Pentaceratops sternbergii* from New Mexico. Journal of Paleontology, **72**: 894–906. doi:10.1017/S0022336000027220.

Lehman, T.M., Wick, S.L., and Barnes, K.R. 2017. New specimens of horned dinosaurs from the Aguja Formation of West Texas, and a revision of *Agujaceratops*. Journal of Systematic Palaeontology, **15**: 641–674. doi:10.1080/14772019.2016.1210683.

Loewen, M.A., Sampson, S.D., Lund, E.K., Farke, A.A., Aguillón-Martinez, M.C., De Leon, C.A., et al. 2010. Horned dinosaurs (Ornithischia: Ceratopsidae) from the Upper Cretaceous (Campanian) Cerro del Pueblo Formation, Coahila, Mexico. *In* New Perspectives on Horned Dinosaurs: The Royal Tyrrell Museum Ceratopsian Symposium. *Edited by* M.J. Ryan, B.J. Chinnery-Allgeier and D.A. Eberth. Indiana University Press, Bloomington. p. 99–116.

Loewen, M.A., Sertich, J.J.W., Sampson, S., O'Connor, J.K., Carpenter, S., Sisson, B., et al. 2024. *Lokiceratops rangiformis* gen. et sp. nov. (Ceratop-

sidae: Centrosaurinae) from the Campanian Judith River Formation of Montana reveals rapid regional radiations and extreme endemism within centrosaurine dinosaurs. PeerJ, **12**: e17224. doi:10.7717/peerj.17224.

Longrich, N.R. 2010. *Mojoceratops perifania*, a new chasmosaurine ceratopsid from the late Campanian of Western Canada. Journal of Paleontology, **84**: 681–694. doi:10.1666/09-114.1.

Longrich, N.R. 2013. *Judiceratops tigris*, a new horned dinosaur from the middle Campanian Judith River Formation of Montana. Bulletin of the Peabody Museum of Natural History, **54**(1): 51–65. doi:10.3374/014.054.0103.

Longrich, N.R. 2014. The horned dinosaurs *Pentaceratops* and *Kosmoceratops* from the upper Campanian of Alberta and implications for dinosaur biogeography. Cretaceous Research, **51**: 292–308. doi:10.1016/j.cretres.2014.06.011.

Lucas, S.G., Sullivan, R.M., and Hunt, A.P. 2006. Re-evaluation of *Pentaceratops* and *Chasmosaurus* (Ornithischia: Ceratopsidae) in the Upper Cretaceous of the Western Interior. New Mexico Museum of Natural History and Science, **35**: 367–370.

Lull, R.S. 1933. A revision of the Ceratopsia or horned dinosaurs. Memoirs of the Peabody Museum of Natural History, **3**(part 3): 1–175.

Maddison, W.P., and Maddison, D.R. 2023. Mesquite: a modular system for evolutionary analysis. Version 3.81. Available from http://www.mesquiteproject.org.

Maidment, S.C.R., and Barrett, P.M. 2011. A new specimen of *Chasmosaurus belli* (Ornithischia: Ceratopsidae), a revision of the genus, and the utility of postcrania in the taxonomy and systematics of ceratopsid dinosaurs. Zootaxa, **296**: 1–47. doi:10.11646/zootaxa.2963.1.1.

Mallon, J.C., Roloson, M., Bamforth, E.L., Scannella, J.B., and Ryan, M.J. 2025. The Canadian fossil record supports anagenesis in *Triceratops* (Ornithischia, Ceratopsia). Canadian Journal of Earth Sciences **62**(7): 1222–1236. doi:10.1139/cjes-2024-0170

Mallon, J.C. 2017. Recognizing sexual dimorphism in the fossil record: lessons from nonavian dinosaurs. Paleobiology, **43**: 495–507. doi:10.1017/pab.2016.51.

Mallon, J.C., Evans, D.C., Ryan, M.J., and Anderson, J.S. 2012. Megaherbivorous dinosaur turnover in the Dinosaur Park Formation (upper Campanian) of Alberta, Canada. Palaeogeography, Palaeoclimatology, Palaeoecology, **350-352**: 124–138. doi:10.1016/j.palaeo.2012.06.024.

Mallon, J.C., Holmes, R., Anderson, J.A., Farke, A.A., and Evans, D.C. 2014. New information on the rare horned dinosaur *Arrhinoceratops brachyops* (Ornithischia: Ceratopsidae) from the Upper Cretaceous of Alberta, Canada. Canadian Journal of Earth Sciences, **51**: 618–634. doi:10.1139/cjes-2014-0028.

Mallon, J.C., Holmes, R., Eberth, D.A., Ryan, M.J., and Anderson, J.S. 2011. Variation in the skull of *Anchiceratops* (Dinosauria, Ceratopsidae) from the Horseshoe Canyon Formation (Upper Cretaceous) of Alberta. Journal of Vertebrate Paleontology, **31**(5): 1047–1071. doi:10.1080/02724634.2011.601484.

Mallon, J.C., Holmes, R.B., and Rufolo, S.J. 2023. Development and homology of the medial parietal ornamentation in centrosaurine ceratopsids (Dinosauria: Ornithischia). Journal of Vertebrate Paleontology, **42**: 1–6. doi:10.1080/02724634.2023.2211638.

Mallon, J.C., Ott, C.J., Larson, P.L., Iuliano, E.M., and Evans, D.C. 2016. *Spiclypeus shipporum* gen. et sp. nov., a boldly audacious new chasmosaurine ceratopsid (Dinosauria: Ornithischia) from the Judith River Formation (Upper Cretaceous: Campanian) of Montana, USA. PLoS ONE, **11**(5): e0154218. doi:10.1371/journal.pone.0154218.

Mallon, J.C., Ryan, M.J., and Campbell, J.A. 2015. Skull ontogeny in *Arrhinoceratops brachyops* (Ornithischia: Ceratopsidae) and other horned dinosaurs. Zoological Journal of the Linnean Society, **175**: 910–929. doi:10.1111/zoj.12294.

Marsh, O.C. 1888. A new family of horned dinosaurs from the Cretaceous. American Journal of Science, **s3-36**: 477–478. doi:10.2475/ajs.s3-36.216.477.

Marsh, O.C. 1889. Notice of a gigantic horned Dinosauria from the Cretaceous. American Journal of Science, **s3-38**: 173–176. doi:10.2475/ajs.s3-38.224.173.

Maryańska, T., and Osmólska, H. 1975. Protoceratopsidae (Dinosauria) of Asia. Palaeontologia Polonica, **33**: 133–182.

Motani, R. 2021. Sex estimation from morphology in living animals and dinosaurs. Zoological Journal of the Linnean Society, **192**: 1029–1044. doi:10.1093/zoolinnean/zlaa181.

Osborn, H.F. 1923. A new genus and species of ceratopsia from New Mexico, *Pentaceratops sternbergii*. American Museum Novitates, **93**: 1–3.

Ostrom, J.H., and Wellnhofer, P. 1986. The Munich specimen of *Triceratops* with a revision of the genus. Zitteliana, **14**: 111–158.

Padian, K., and Horner, J.R. 2011. The evolution of 'bizarre structures' in dinosaurs: biomechanics, sexual selection, social selection or species recognition? Journal of Zoology, **283**: 3–17. doi:10.1111/j.1469-7998.2010.00719.x.

Pintor, R., Cornette, R., Houssaye, A., and Allain, R. 2023. Femora from an exceptionally large population of coeval ornithomimosaurs yield evidence of sexual dimorphism in extinct theropod dinosaurs. Elife, **12**: e83413. doi:10.7554/eLife.83413.

Prieto-Márquez, A., Garcia-Porta, J., Joshi, S.H., Norell, M.A., and Makovicky, P.J. 2020. Modularity and heterochrony in the evolution of the ceratopsian dinosaur frill. Ecology and Evolution, **10**: 6288–6309. doi:10.1002/ece3.6361.

Ramezani, J., Beveridge, T.L., Rogers, R.R., Eberth, D.A., and Roberts, E.M. 2022. Calibrating the zenith of dinosaur diversity in the Campanian of the Western Interior Basin by CA-ID-TIMS U–Pb geochronology. Scientific Reports, **12**: 16026. doi:10.1038/s41598-022-19896-w.

Rowe, T., Colbert, E.H., and Nations, J.D. 1981. The occurrence of *Pentaceratops* (Ornithischia: Ceratopsia) with a description of its frill. *In* Advances in San Juan Basin Paleontology. *Edited by* S.G. Lucas, K. Rigby and B. Kues. University of New Mexico Press, Albuquerque, US. p. 29–48.

Ryan, M.J., and Evans, D.A. 2005. Ornithischian dinosaurs. *In* Dinosaur Provincial Park: A Spectacular Ancient Ecosystem Revealed. *Edited by* P.J. Currie and E.B. Koppelhus. Indiana University Press, Bloomington, Indiana. p. 312–348.

Ryan, M.J., Russell, A.P., Eberth, D.A., and Currie, P.J. 2001. The taphonomy of a *Centrosaurus* (Ornithischia: Ceratopsidae) bone bed from the Dinosaur Park Formation (Upper Campanian), Alberta, Canada, with comments on cranial ontogeny. Palaios, **16**(5): 482–506. doi:10.1669/0883-1351(2001)016⟨0482:TTOACO⟩2.0.CO;2.

Saitta, E.T., Stockdale, M.T., Longrich, N.R., Bonhomme, V., Benton, M.J., Cuthill, I.C., and Makovicky, P.J. 2020. An effect size statistical framework for investigating sexual dimorphism in non-avian dinosaurs and other extinct taxa. Biological Journal of the Linnean Society, **131**: 231–273. doi:10.1093/biolinnean/blaa105.

Sampson, S.D., Loewen, M.A., Farke, A.A., Roberts, E.M., Forster, C.A., Smith, J.A., and Titus, A.L. 2010. New horned dinosaurs from Utah provide evidence for intracontinental dinosaur endemism. PLoS ONE, **5**(9): e12292. doi:10.1371/journal.pone.0012292.

Sampson, S.D., Ryan, M.J., and Tanke, D.H. 1997. Craniofacial ontogeny in centrosaurine dinosaurs (Ornithischia: Ceratopsidae): taxonomic and behavioral implications. Zoological Journal of the Linnean Society, **121**: 293–337. doi:10.1111/j.1096-3642.1997.tb00340.x.

Scannella, J.B., Fowler, D.W., Goodwin, M.B., and Horner, J.R. 2014. Evolutionary trends in *Triceratops* from the Hell Creek Formation, Montana. Proceedings of the National Academy of Sciences, **111**: 10245–10250. doi:10.1073/pnas.1313334111.

Sereno, P.C. 1986. Phylogeny of the bird-hipped dinosaurs (Order Ornithischia). National Geographic Research, **2**: 234–256.

Sternberg, C.M. 1929. A new species of horned dinosaur from the Upper Cretaceous of Alberta. National Museum of Canada Bulletin, **54**: 34–37.

Sternberg, C.M. 1940. Ceratopsidae from Alberta. Journal of Paleontology, **14**: 468–480.

Wolfe, D.G., and Kirkland, J. 1998. *Zuniceratops christopheri* n. gen. & n. sp., a new ceratopsid dinosaur from the Moreno Hill Formation (Cretaceous, Turonian) of west-central New Mexico. New Mexico Museum of Natural History and Science Bulletin, **14**: 303–317.